Acta Cryst B
STRUCTURAL SCIENCE
CRYSTAL ENGINEERING
MATERIALS

April 2022 issue

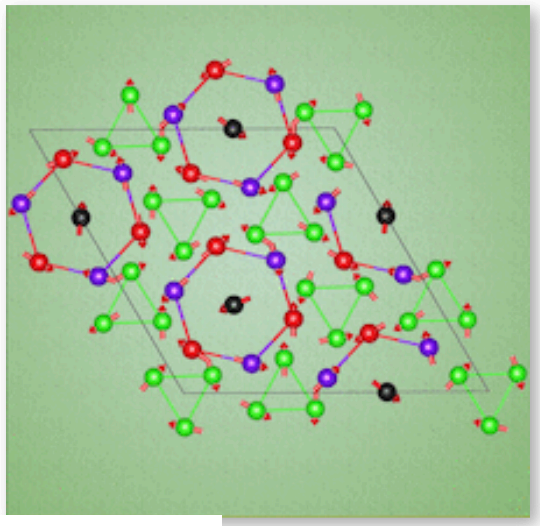

Cover illustration View of the magnetic Tb atoms of antiferrom
P6′ symmetry [see Pomjakushin *et al.* (2022). *Acta Cryst.* B**78**, 1

# Revisiting the antiferromagnetic structure of $Tb_{14}Ag_{51}$: the importance of distinguishing alternative symmetries for a multidimensional order parameter

**Vladimir Pomjakushin,[a]* Juan Manuel Perez-Mato,[b] Peter Fischer,[a] Lukas Keller[a] and Wiesława Sikora[c]**

[a]Laboratory for Neutron Scattering and Imaging (LNS), Paul Scherrer Institut (PSI), CH-5232 Villigen, Switzerland, [b]Facultad de Ciencia y Tecnologa, Universidad del Pas Vasco, UPV/EHU, Apartado 644, E-48080 Bilbao, Spain, and [c]Faculty of Physics and Applied Computer Science, AGH University of Science and Technology, PL-30-059 Krakow, Poland. *Correspondence e-mail: vladimir.pomjakushin@psi.ch

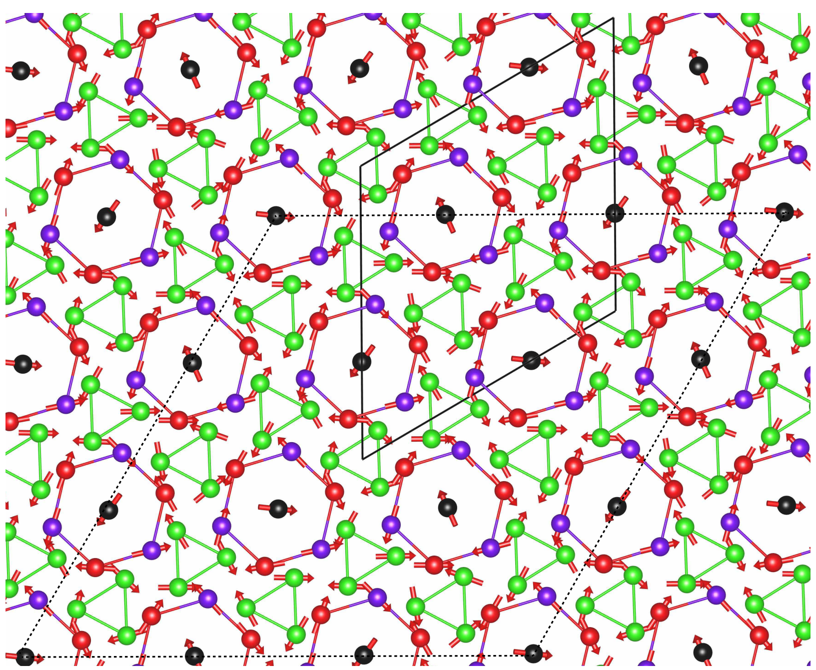

https://onlinelibrary.wiley.com/iucr/doi/10.1107/S205252062200124X#

# Plan

- History behind the paper
  - Initial motivation to study magnetic structure of $Tb_{14}Ag_{51}$
  - First experiments Saphir – 1990
  - Experiments at SINQ DMC and HRPT – 2004

  - Magnetic structure published in 2006

  - Manuel Perez−Mato idea: high symmetry lost 2014−,…2019

# Plan

- History behind the paper
  - Initial motivation to study magnetic structure of $Tb_{14}Ag_{51}$
  - First experiments Saphir – 1990
  - Experiments at SINQ DMC and HRPT – 2004

  - Magnetic structure published in 2006

  - Manuel Perez–Mato idea: high symmetry lost 2014–,…2019

- Herring criterion of the irreducible representations (irrep) type. Complex irreps.
- Alternative symmetries in case of multi-dim irreps

# Plan

- History behind the paper
  - Initial motivation to study magnetic structure of $Tb_{14}Ag_{51}$
  - First experiments Saphir – 1990
  - Experiments at SINQ DMC and HRPT – 2004

  - Magnetic structure published in 2006

  - Manuel Perez–Mato idea: high symmetry lost 2014–,…2019

- Herring criterion of the irreducible representations (irrep) type. Complex irreps.
- Alternative symmetries in case of multi-dim irreps

- Neutron diffraction: new much better model for magnetic structure of $Tb_{14}Ag_{51}$

# Initial motivation to study Tb14Ag51 in 1990…

Hexagonal P6/m space group

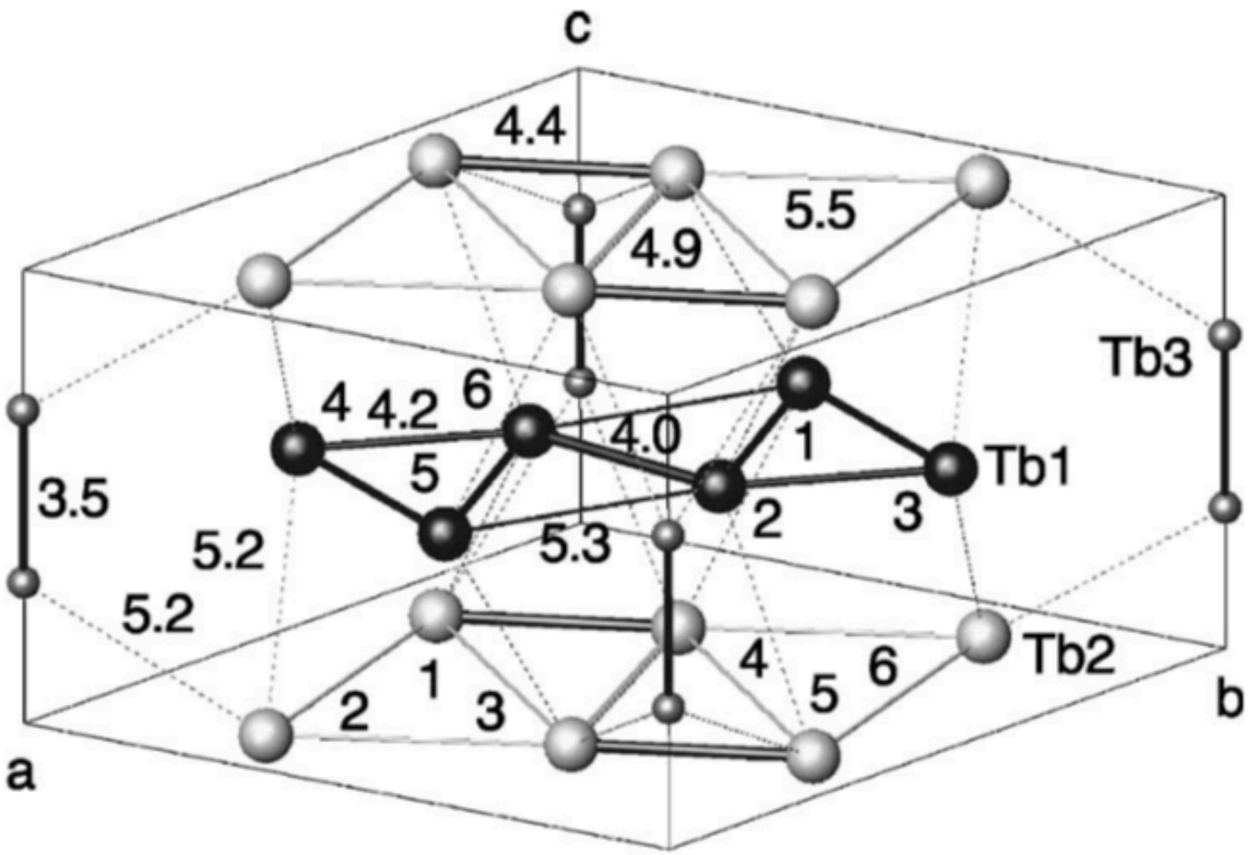


| | |
|---|---|
| Tb1 | 6*k* |
| Tb2 | 6*j* |
| Tb3 | 2*e* |

In actinides $U_{14}Au_{51}$ the f−electrons which carry the magnetism can participate in the Fermi surface

⇓

complex electronic properties like heavy−fermion behaviour, superconductivity and antiferromagnetism (AFM).

?

In which extent AFM ordering is different in $Tb_{14}Ag_{51}$ and in particular to investigate whether there may be also magnetic order on all rare−earth sites?

# Interesting features of geometrically frustrated Tb14Ag51

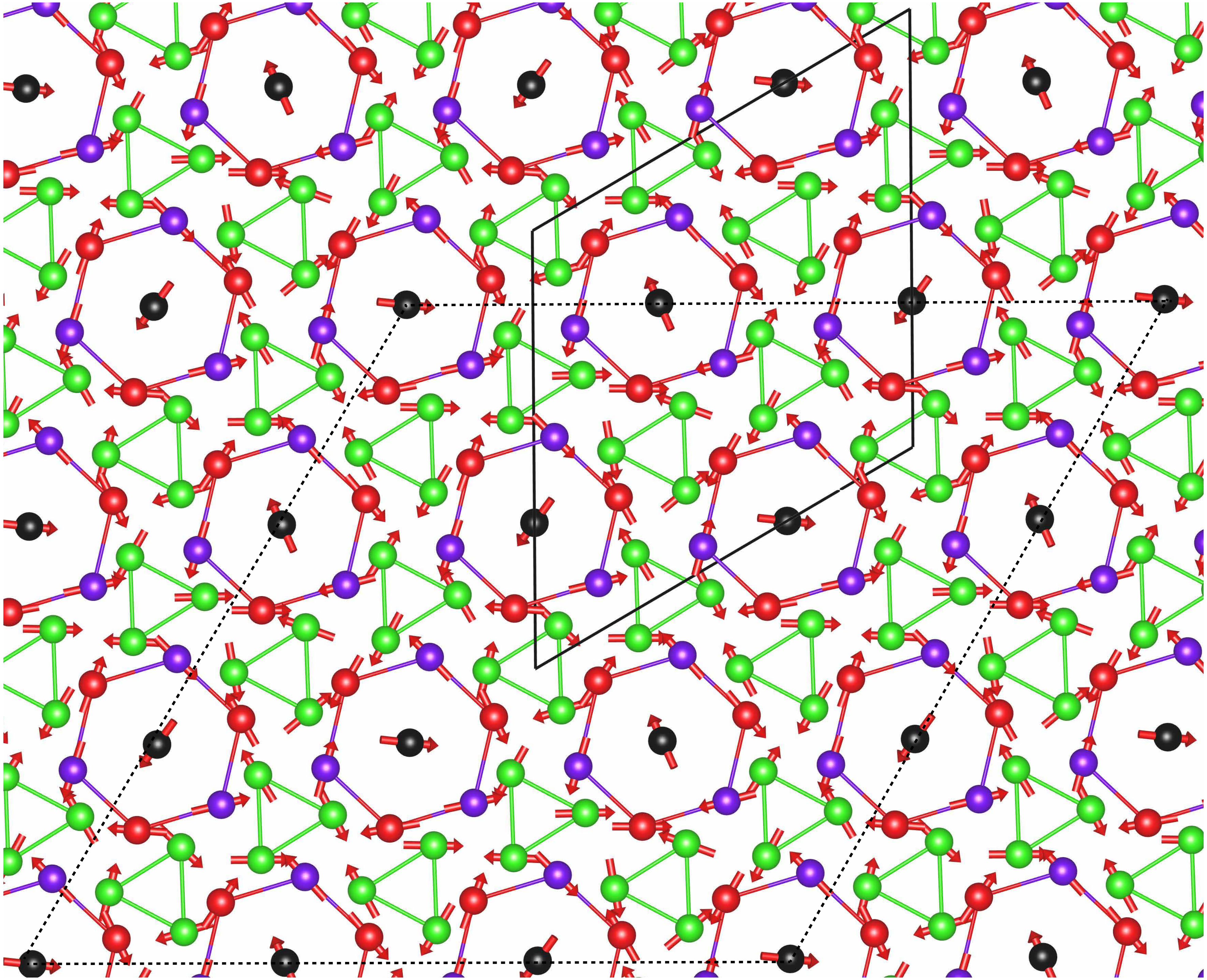

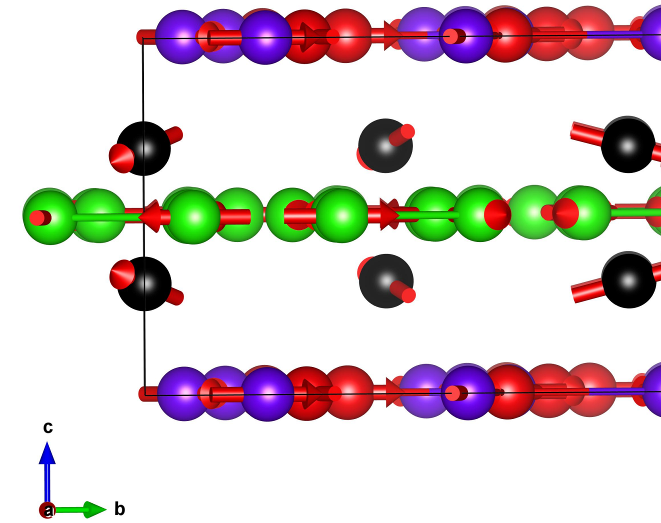

# Interesting features of geometrically frustrated Tb14Ag51

- Textbook-like example of distinguishing alternative symmetries for VERY complex magnetic structure: 27 parameters, 15 if M=const. (78 if only irreps without symmetry).

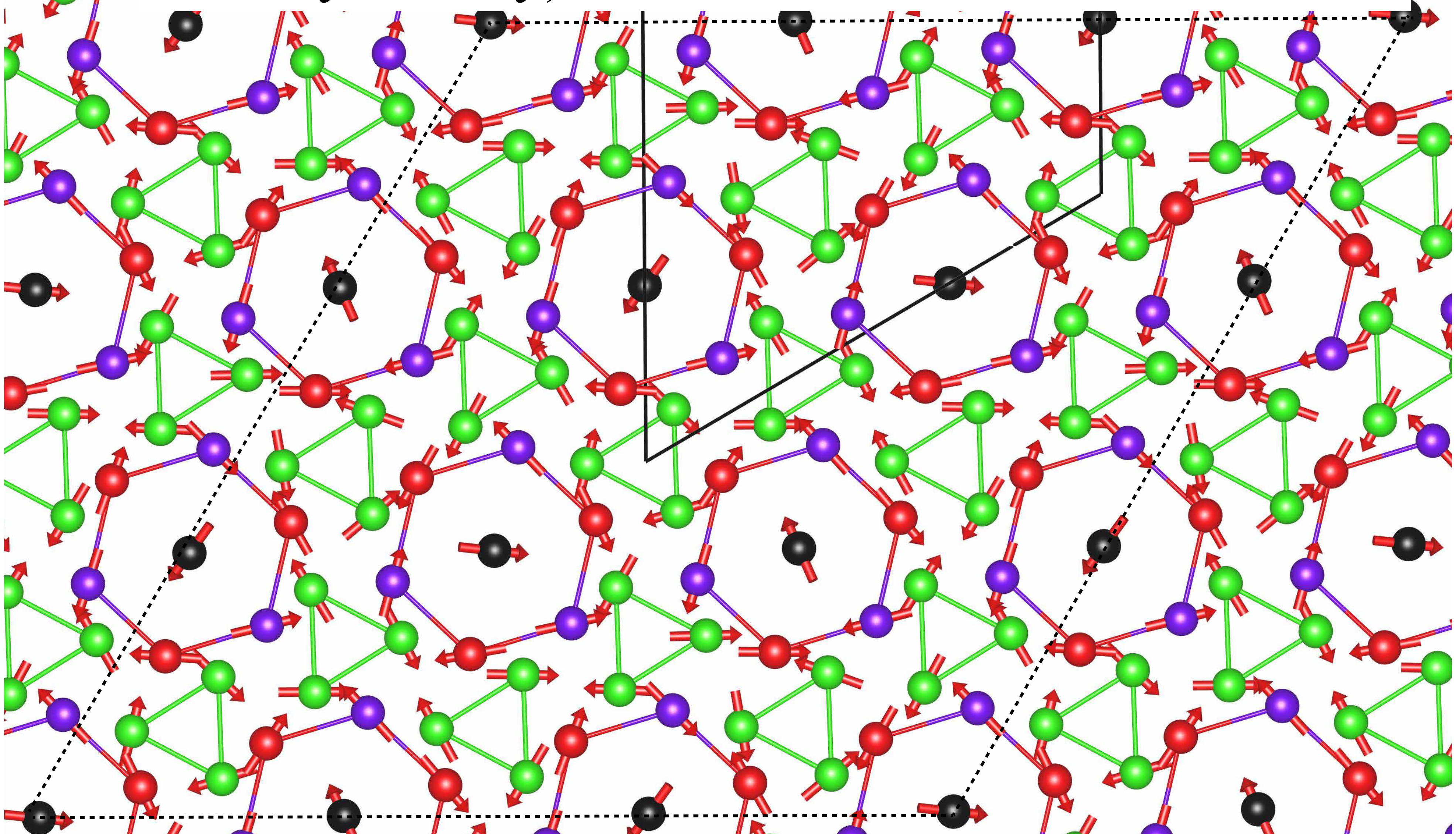

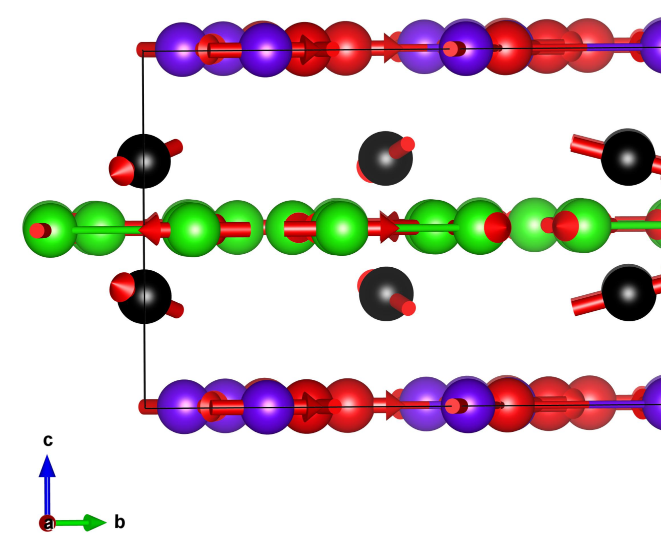

# Comparison of magnetic & nuclear scattering lengths

| Comparison of neutron scattering lengths (fm) | | | |
|---|---|---|---|
| **magnetic** | | | |
| Tb (~ 8.5μB): | −23, | $Cu^{2+}$ (S=½): −2.65 | |
| **nuclear** | | | **smallest** |
| Tb : | +7, | Ag: +7.7 | V: −0.4, Li: −1.9 |

fm=fermi=$10^{-13}$ cm

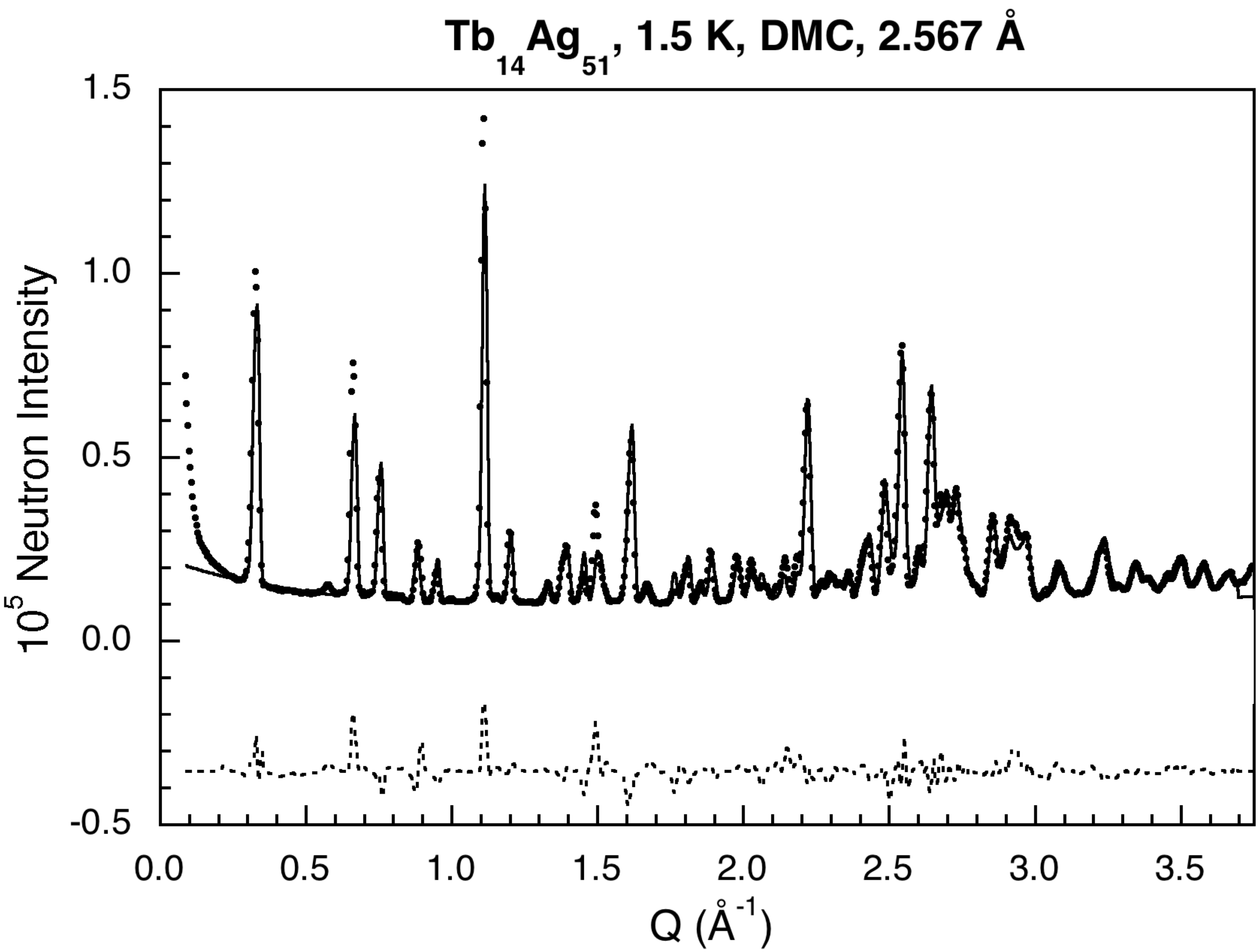
Tb14Ag51, 1.5 K, DMC, 2.567 Å
10^5 Neutron Intensity
Q (Å^-1)
1.5
1.0
0.5
0.0
-0.5
0.0
0.5
1.0
1.5
2.0
2.5
3.0
3.5

# magnetic scattering intensity is larger than the nuclear one

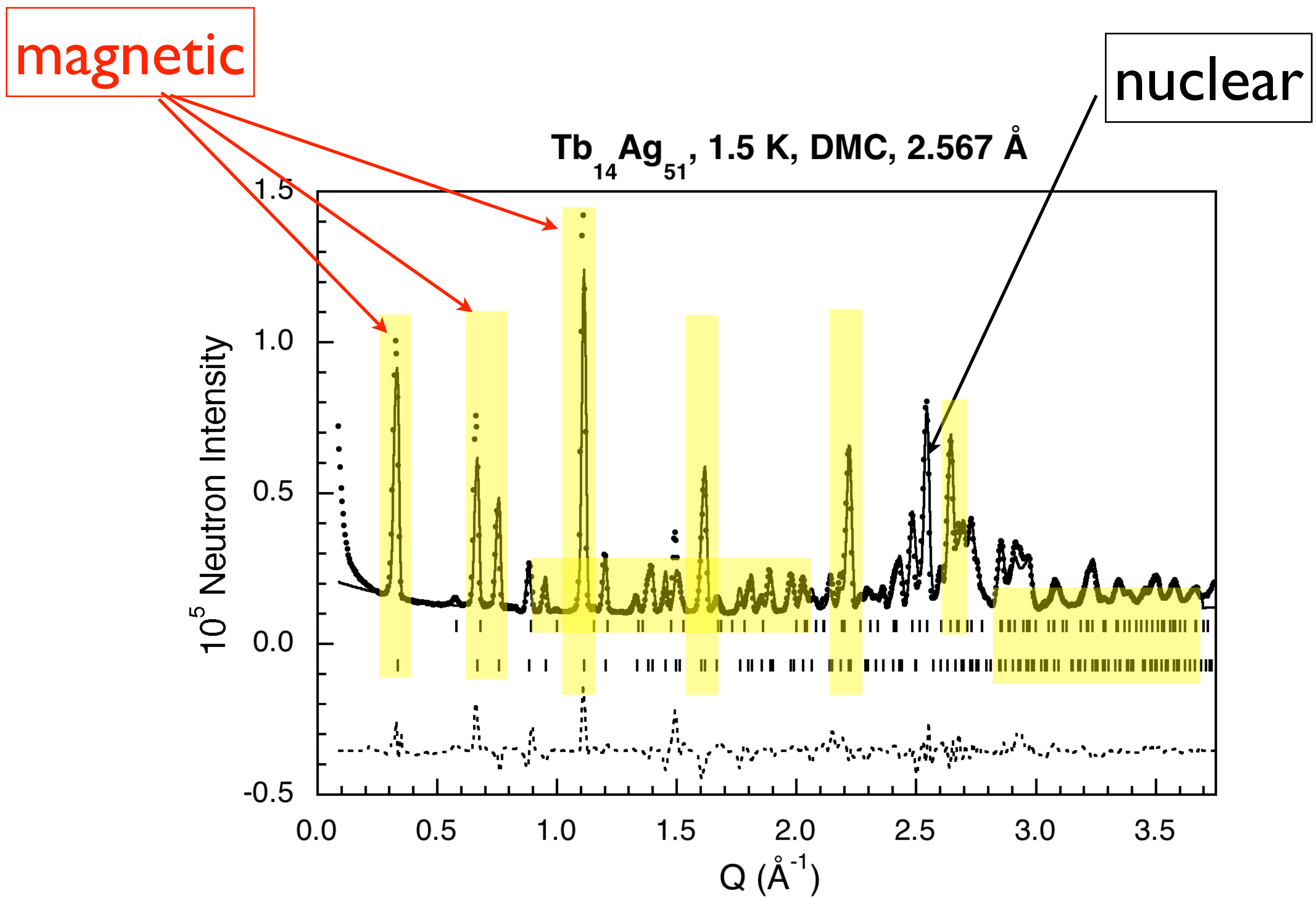

# Interesting features of geometrically frustrated Tb14Ag51

- Textbook-like example of VERY complex magnetic structure: 27 parameters, 15 if M=const.

- spontaneous electric polarization induced by a noncollinear AFM ordering

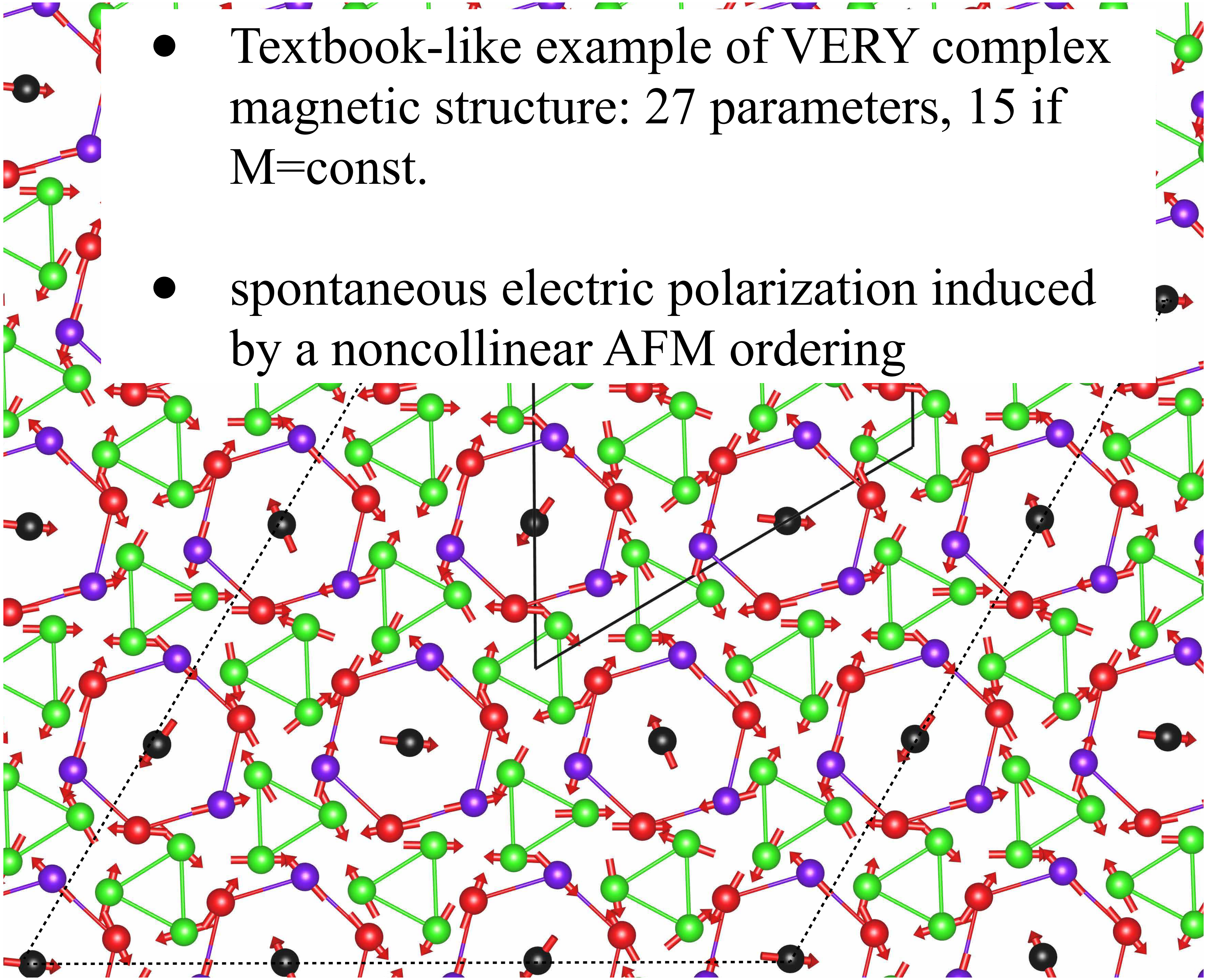

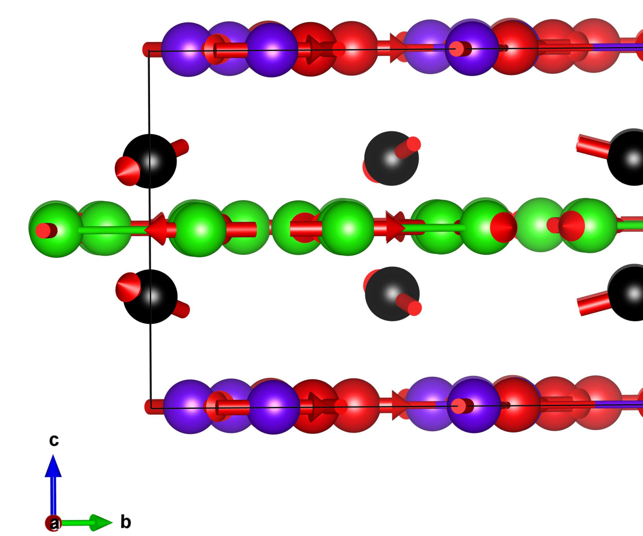

# Interesting features of geometrically frustrated Tb14Ag51

- Textbook-like example of VERY complex magnetic structure: 27 parameters, 15 if M=const.

- spontaneous electric polarization induced by a noncollinear AFM ordering

  Vortex spin configuration allows exotic multipoles★ (important for spintronics):

- ferroic time-reversal-odd polar-tensor quantities, like ferromagnetic toroidicity (**r** x **M**)
- ferroaxial moment with time-reversal even and space inversion even (**r** x **Q**)

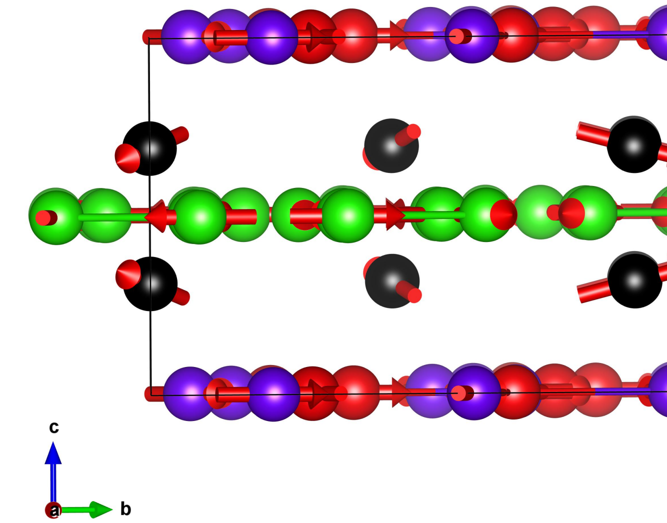


★ Satoru Hayami, PHYSICAL REVIEW B 106, 144402 (2022)

The materials hosting the vortex spin configurations in in some specific symmetries with exotic multipoles

CH9100207

**Labor für Neutronenstreuung**

**ETH Zürich**

# Neutronen-Streuung
# (Progress Report)
# Januar - Dezember 1990

**LNS-154**

**Februar 1991**

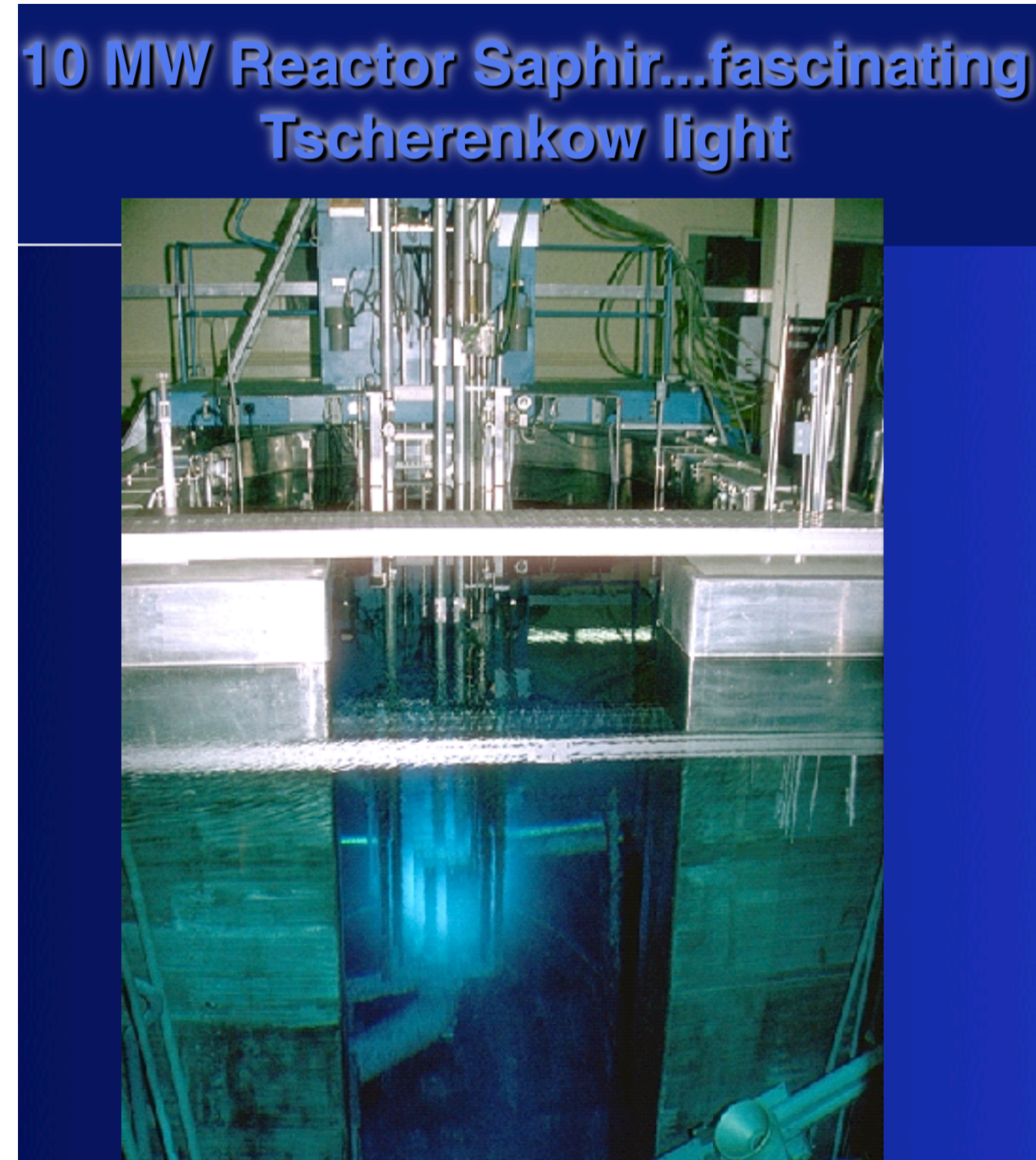


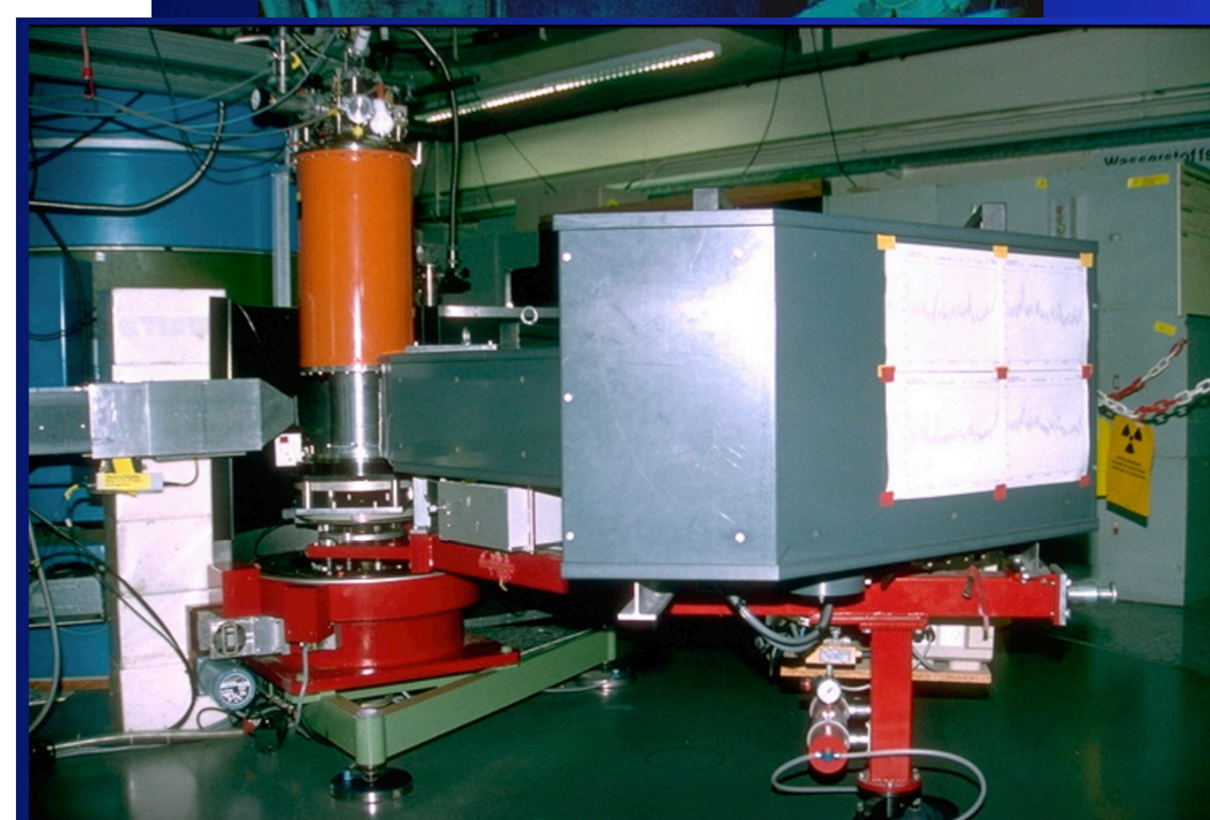

## 4.8 THE CRYSTAL STRUCTURE AND THE MAGNETIC ORDER OF $Tb_{14}Ag_{51}$

A. Dommann[1], P. Fischer[2] and F. Hulliger[1]
[1]Laboratorium für Festkörperphysik, ETH, CH–8093 Zürich (Switzerland)
[2]Labor für Neutronenstreuung, ETH, CH–5232 Villigen PSI (Switzerland)

The present study on $Tb_{14}Ag_{51}$ was prompted by our investigations on isostructural $U_{14}Au_{51}$. The absence of additional purely magnetic peaks in the neutron diffraction pattern of $U_{14}Au_{51}$ led to a set of U atoms in position 2e with no contributions to the magnetic ordering [1]. In a compound with the same $Gd_{14}Ag_{51}$ type structure but consisting of atoms with larger magnetic moments and on which the magnetic moment cannot be quenched as in $U_{14}Au_{51}$ additional purely magnetic peaks have to occur. As an example of latter type we chose $Tb_{14}Ag_{51}$ owing to the favorable properties of Tb. At low temperatures we found indeed the expected purely magnetic peaks in the neutron diffraction pattern of $Tb_{14}Ag_{51}$.

Polycrystalline samples of $Tb_{14}Ag_{51}$ were prepared in the same way as $U_{14}Au_{51}$ as described in ref. [2]. Under the microscope the polycrystalline samples appeared to be homogeneous and no lines due to foreign phases were detectable on the X-ray diffraction patterns.

The crystal structure of $Tb_{14}Ag_{51}$ was determined at room temperature and at 10 K by means of a Rietveld analysis of the X-ray powder diffraction intensities. $Tb_{14}Ag_{51}$ shows a Curie–Weiss-type susceptibility with a peak at 27 K, indicating antiferromagnetic ordering. Specific-heat data also reveal a small anomaly at 27 K.

Powder neutron-diffraction measurements were performed on the multidetector powder

magnetic data were derived. The crystal structure is of the hexagonal $Gd_{14}Ag_{51}$ type (space group *P* 6/*m*) in the whole temperature range from 1 K to 295 K. The additional purely magnetic Bragg peaks on our 1 K neutron diffraction pattern correspond to $\vec{k}$ = [1/3, 1/3, 0]. The evaluation of the detailed magnetic structure is in progress.

### References

[1] A. Dommann, H.R. Ott, F. Hulliger and P. Fischer, *J. Less-Common Met.* ***160***, 171 (1990).

[2] H.R. Ott, E. Felder, A. Schilling, A. Dommann and F. Hulliger, *Solid State Commun.* ***71***, 549 (1989).

PHYSICAL REVIEW B **72**, 134413 (2005)

# Antiferromagnetic three-sublattice Tb ordering in $Tb_{14}Ag_{51}$

P. Fischer,[1,*] V. Pomjakushin,[1] L. Keller,[1] A. Daoud-Aladine,[1] W. Sikora,[2] A. Dommann,[3,†] and F. Hulliger[3]

[1]*Laboratory for Neutron Scattering, ETH Zurich & Paul Scherrer Institute, CH-5232 Villigen PSI, Switzerland*

[2]*Faculty of Physics and Applied Computer Science, AGH University of Science and Technology, PL-30-059 Krakow, Poland*

[3]*Laboratory for Solid State Physics, ETH Hönggerberg, CH-8093 Zurich, Switzerland*

(Received 23 March 2005; revised manuscript received 16 May 2005; published 12 October 2005)

Bulk magnetic, x-ray, and neutron-diffraction measurements were performed on polycrystalline $Tb_{14}Ag_{51}$ in the temperature range from 1.5 K to room temperature. Its chemical $Gd_{14}Ag_{51}$-type structure corresponding to space group $P6/m$ has been refined at 300 and at 30 K. Combined with group-theoretical symmetry analysis, we show that the magnetic structure of this intermetallic compound is of a different $\mathbf{k}=(1/3,1/3,0)$ type with three magnetic Tb sublattices ordering simultaneously below $T_N=27.5(5)$ K according to the combined irreducible representations $\tau_4$ and $\tau_6$.

DOI: 10.1103/PhysRevB.72.134413 PACS number(s): 75.25.+z, 61.12.Ld, 71.20.Eh

## I. INTRODUCTION

Intermetallic uranium and rare-earth $A_{14}B_{51}$ compounds with $Gd_{14}Ag_{51}$ structure[1] have interesting physical properties such as coexistence of antiferromagnetic order and heavy-fermion behavior in $Ce_{14}X_{51}$ ($X$=Au, Ag, Cu),[2] and in $U_{14}Au_{51}$.[3–5] This is related to the fact that there are three crystallographically distinct $A$ sites in this structure.

Moreover, its particular hexagonal symmetry, due to quasitriangular arrangement of magnetic ions, gives rise to considerable geometric frustrations in the magnetic interactions.

diffraction data and performed a careful analysis of both the chemical and magnetic structures of $Tb_{14}Ag_{51}$. In particular we shall prove that in $Tb_{14}Ag_{51}$ the magnetic ordering is of a different type in the important class of intermetallic $A_{14}B_{51}$ compounds with remarkable variation of physical properties. In contrast to the heavy fermion system $U_{14}Au_{51}$,[4] in $Tb_{14}Ag_{51}$ all three $A$ sublattices are shown to order magnetically below $T_N=27.5(5)$ K.

We also measured zero-field $\mu$SR spectra of the powder sample of $Tb_{14}Ag_{51}$ at the GPS spectrometer of Paul Scherrer Institute at 5, 20, and at 30 K. Unfortunately, in contrast to

# magnetic susceptibility and I(T)

k−vector: $k_K$=[1/3, 1/3, 0]

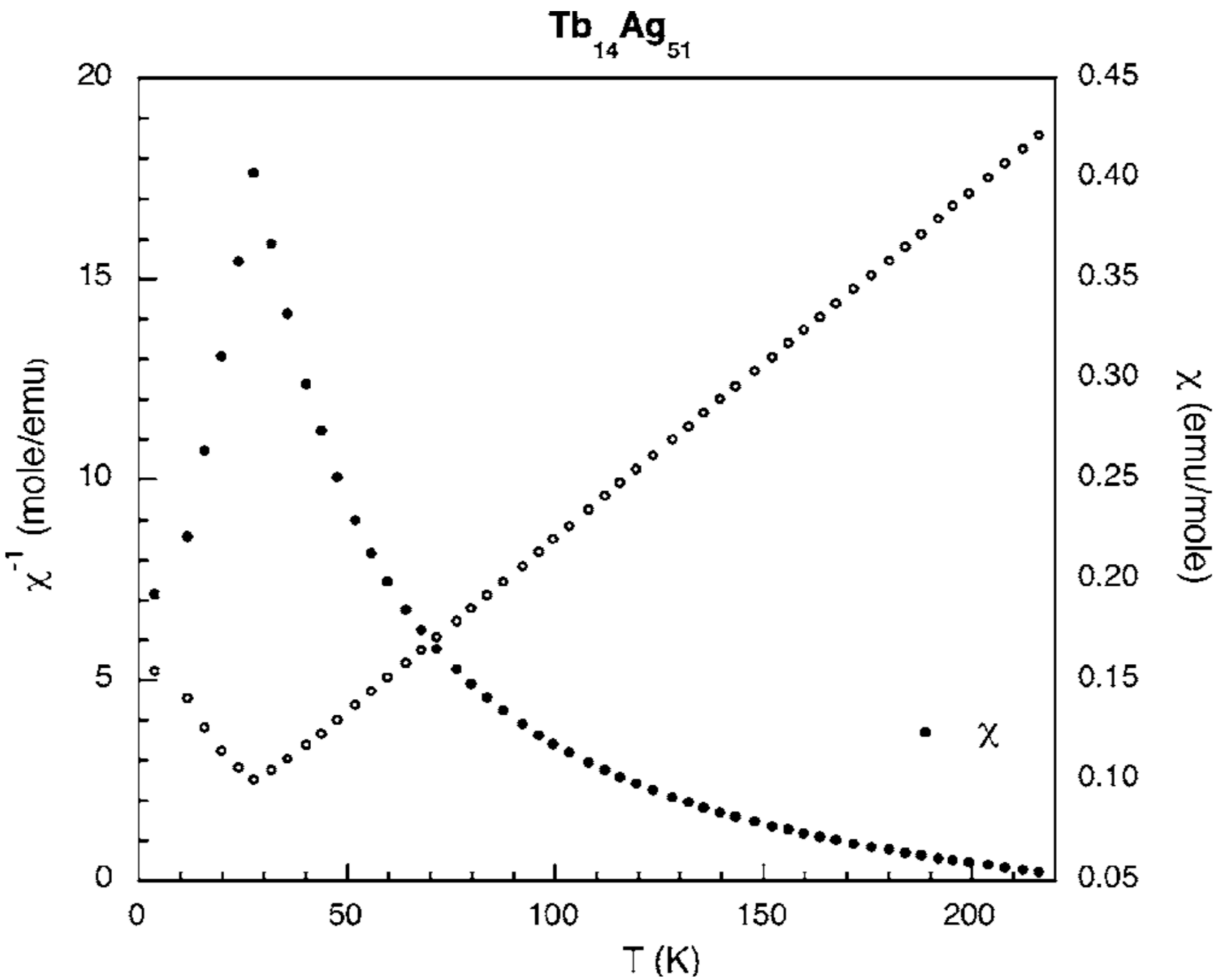


9.67$\mu_B$ / Tb was found to be close to the free ion value
9.72$\mu_B$ / Tb of $Tb^{3+}$ with $^7F_6$ ground state.

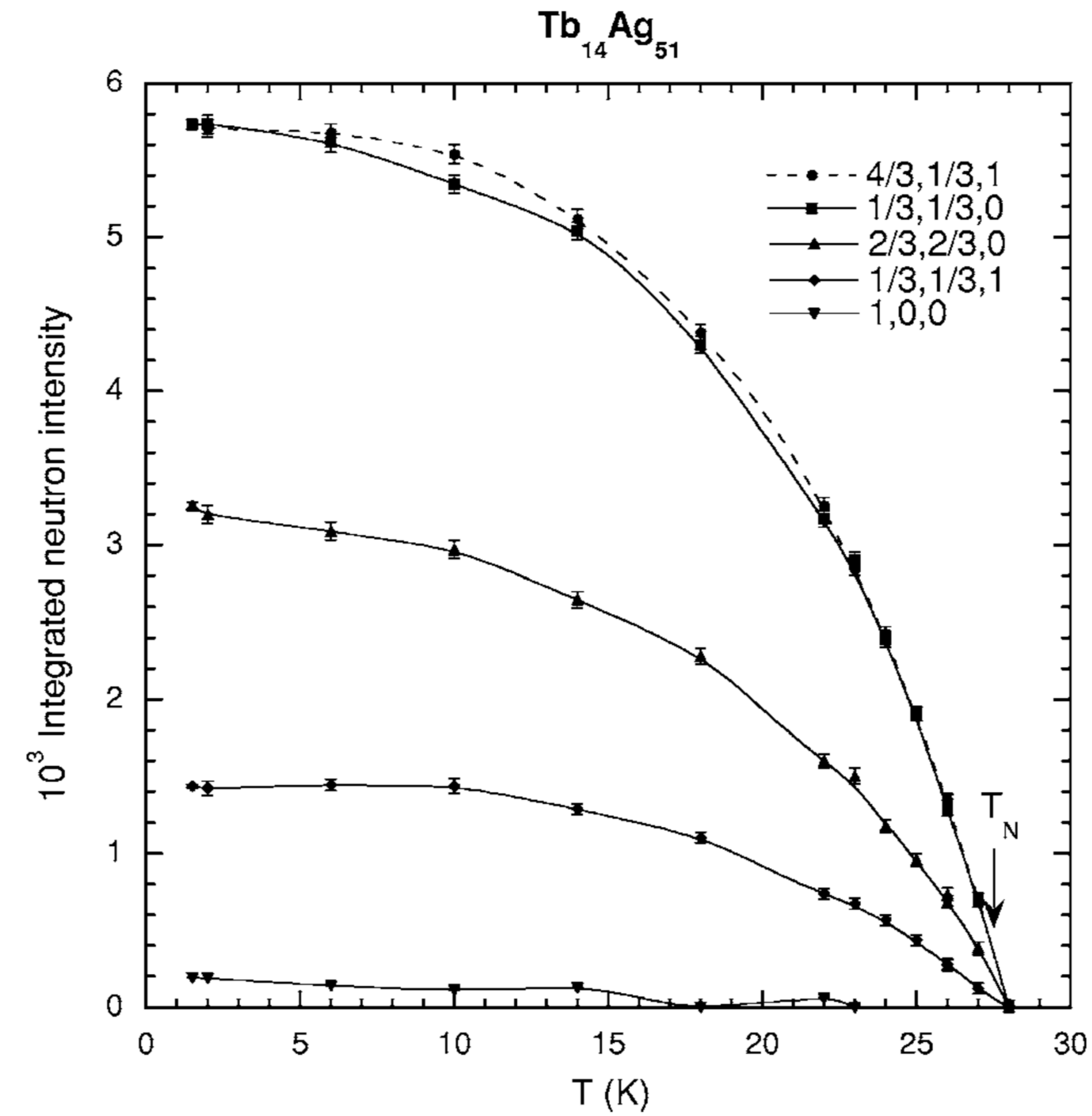


FIG. 5. Temperature dependences of the integrated magnetic neutron intensities of characteristic magnetic Bragg peaks of $Tb_{14}Ag_{51}$. The smooth curves are a guide to the eyes.

# 2k magnetic structure was missed using RA

Antiferromagnetic (à la cycloidal spiral) three sub−lattice ordering in $Tb_{14}Ag_{51}$

P6/m → Pm’ (lowest monoclinic symmetry)

k−vector: $k_K$=[1/3, 1/3, 0]

PHYSICAL REVIEW B 72, 134413 (2005)

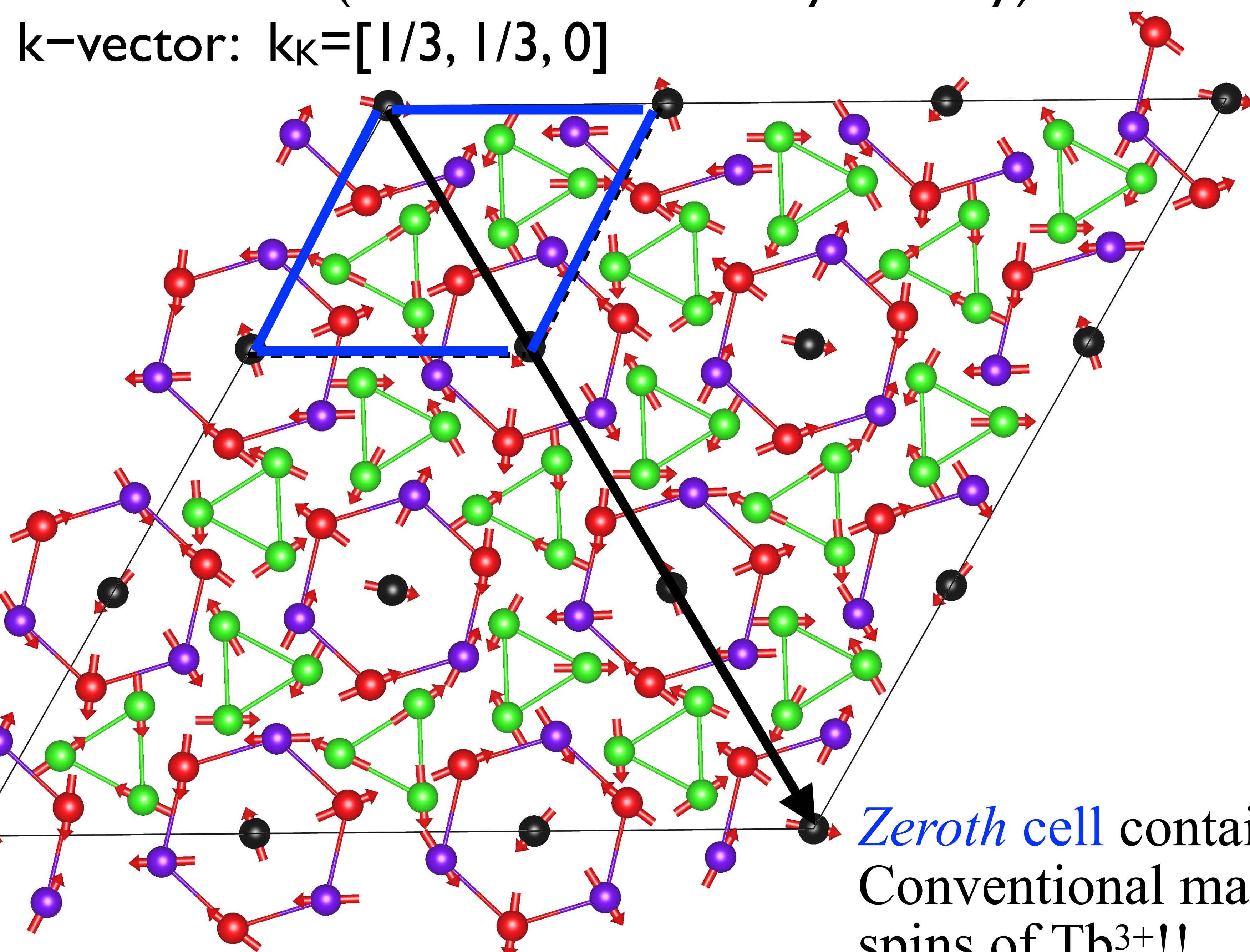

*Zeroth* cell contains 13 spins of $Tb^{3+}$.
Conventional magnetic unit cell contains 126 spins of $Tb^{3+}$!!

# 2k magnetic structure was missed using RA

Antiferromagnetic (à la cycloidal spiral) three sub−lattice ordering in $Tb_{14}Ag_{51}$

P6/m → Pm' (lowest monoclinic symmetry)

k−vector: $k_K$=[1/3, 1/3, 0]

PHYSICAL REVIEW B 72, 134413 (2005)

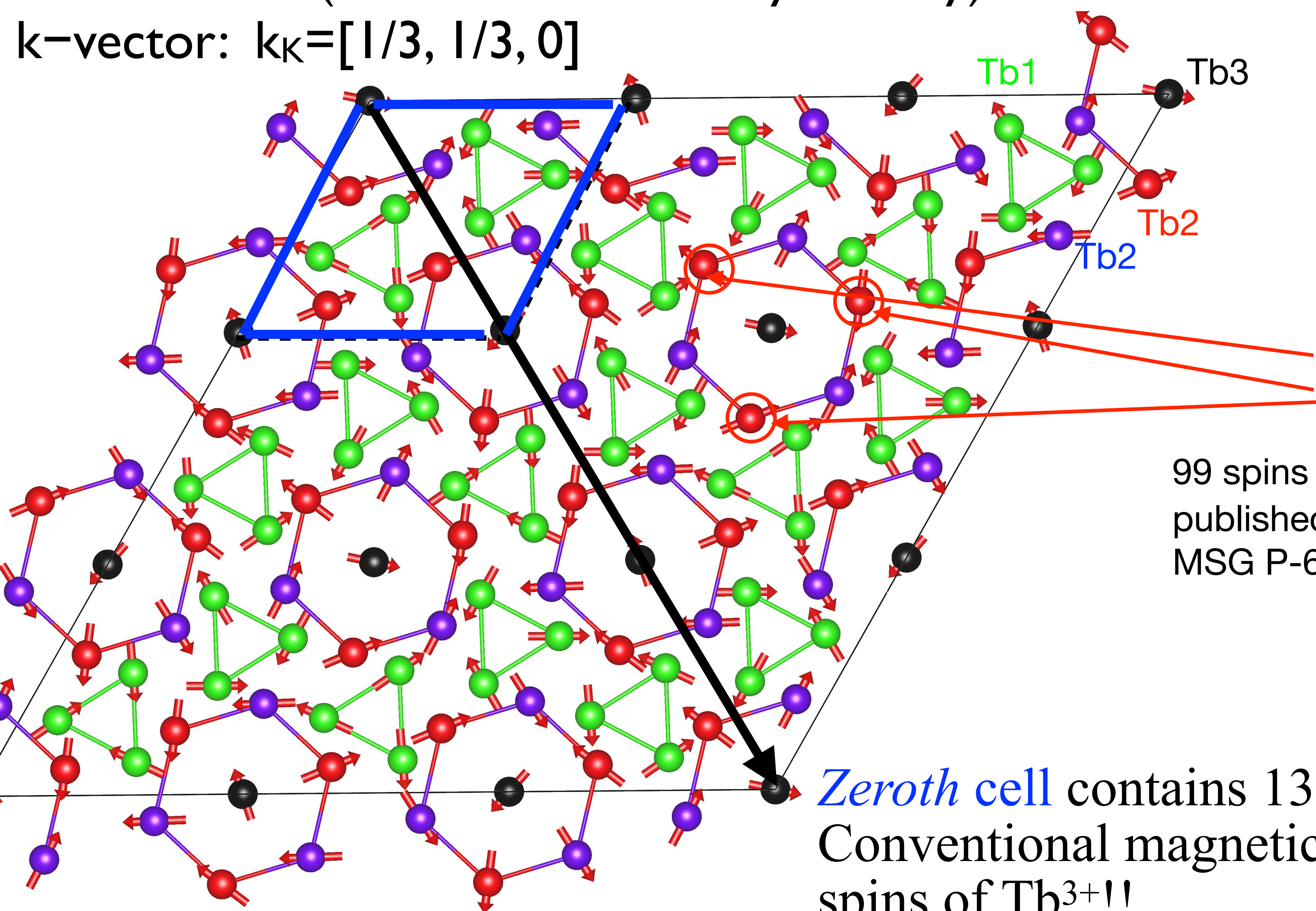


Manuel Perez Mato

Only three of 13 independent sites are “wrong” => Pm’

99 spins in the 3 x 3 x 1 cell of the published model comply with the MSG P-6’, while 27 do not.

*Zeroth* cell contains 13 spins of $Tb^{3+}$. Conventional magnetic unit cell contains 126 spins of $Tb^{3+}$!!

# 2k magnetic structure was missed using RA

Antiferromagnetic (à la cycloidal spiral) three sub−lattice ordering (irrep K4K6) in $Tb_{14}Ag_{51}$

P6/m → Pm' (lowest monoclinic symmetry)

k−vector: $k_K$=[1/3, 1/3, 0]

PHYSICAL REVIEW B 72, 134413 (2005)

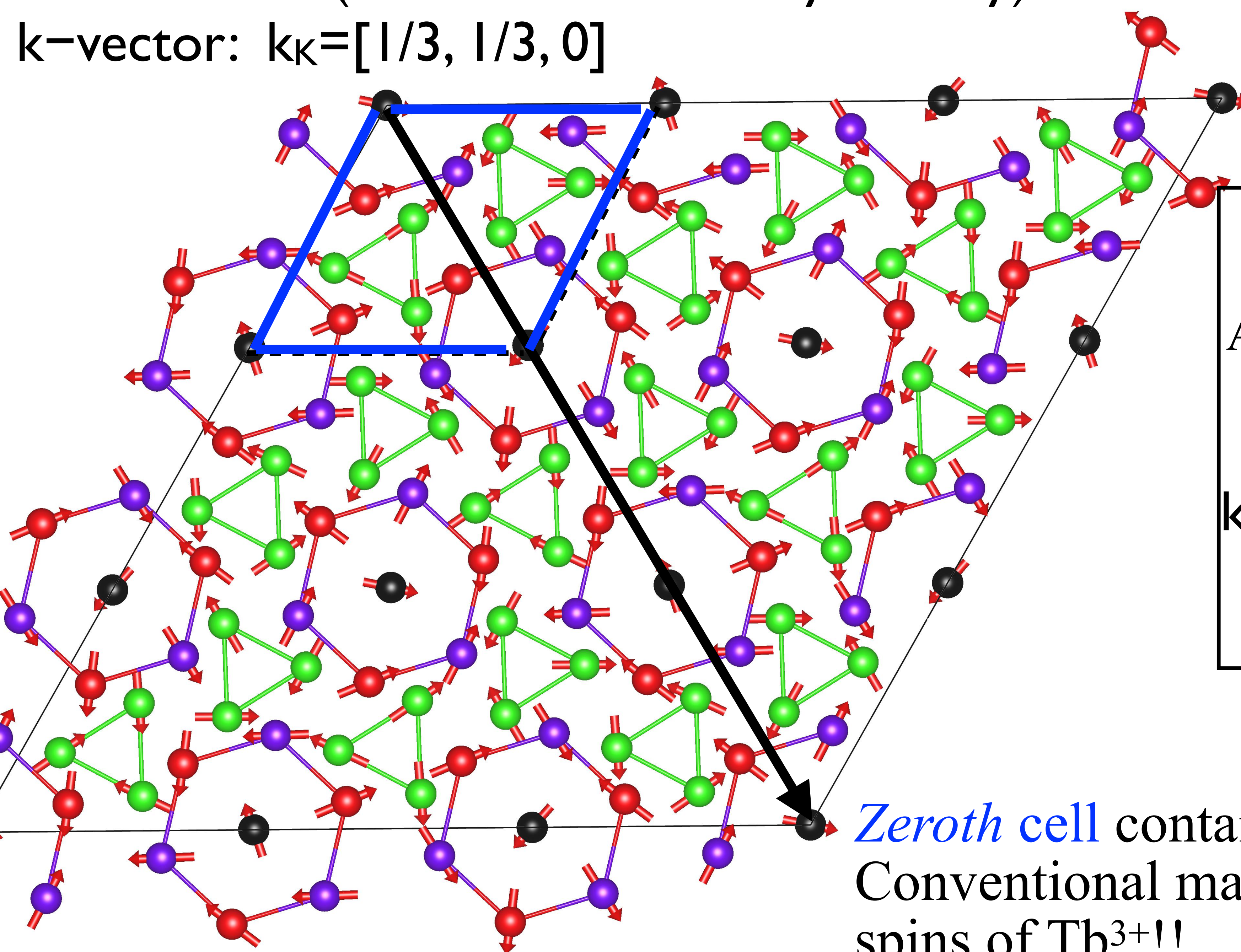

maximal possible symmetry for 4D irrep

Acta Cryst. (2022). B**78**, 172-178

P6/m → P-6'

k−vectors: $k_K$=[1/3, 1/3, 0] and $3k_K$=[0,0,0]

*Zeroth* cell contains 13 spins of $Tb^{3+}$. Conventional magnetic unit cell contains 126 spins of $Tb^{3+}$!!

# Energy Bands of Crystals and Types of irreps.

Conyers Herring

Herring in 1959

Wigner in 1963

AUGUST 15, 1937 PHYSICAL REVIEW VOLUME 52

## Effect of Time-Reversal Symmetry on Energy Bands of Crystals

CONYERS HERRING
*Princeton University, Princeton, New Jersey*
(Received June 16, 1937)

UST 15, 1937 PHYSICAL REVIEW V

## Accidental Degeneracy in the Energy Bands of Crystals

CONYERS HERRING
*Princeton University, Princeton, New Jersey*
(Received June 16, 1937)

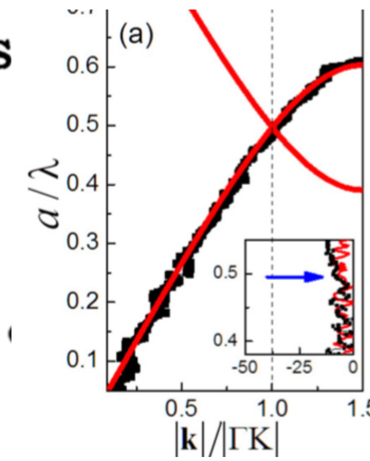


PhysRevB.89.134302

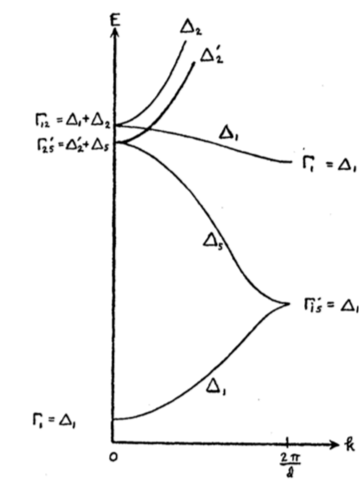


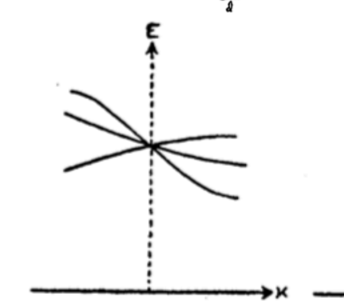


(A)

E. Wigner: The degeneracies, such as touching or crossing the branches, are connected with the properties of the irreps of the spatial symmetry group of the Hamiltonian.
**Three types of irreps – real & two complex.**

*C. Herring PhD thesis: "On Energy Coincidences in the Theory of Brillouin Zones"* (1937) under supervision of Eugene Wigner

# Energy Bands of Crystals and Types of irreps.

Conyers Herring

Herring in 1959

AUGUST 15, 1937 PHYSICAL REVIEW VOLUME 52

## Effect of Time-Reversal Symmetry on Energy Bands of Crystals

CONYERS HERRING
*Princeton University, Princeton, New Jersey*
(Received June 16, 1937)

GUST 15, 1937 PHYSICAL REVIEW V

## Accidental Degeneracy in the Energy Bands of Crystals

CONYERS HERRING
*Princeton University, Princeton, New Jersey*
(Received June 16, 1937)

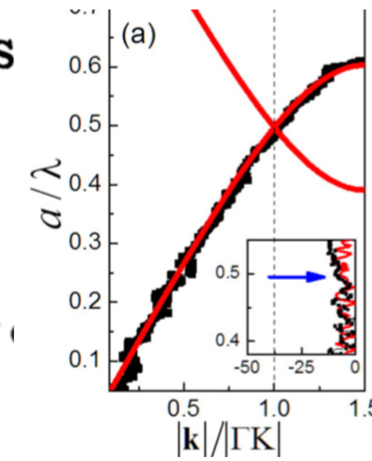


PhysRevB.89.134302

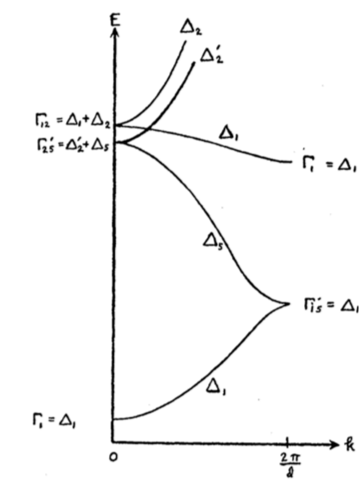

E. Wigner: The degeneracies, such as touching or crossing the branches, are connected with the properties of the irreps of the spatial symmetry group of the Hamiltonian.
**Three types of irreps – real & two complex.**

Wigner in 1963

if H is real:
$E(\psi) = E(\psi^*)$

$\psi \to \psi^*$
is to be interpreted as
|same state>
Alice x,y,z → Bob x,y,z
t → –t

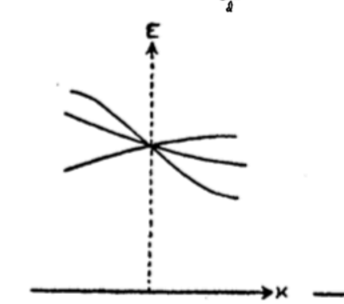

(A)

*C. Herring PhD thesis: "On Energy Coincidences in the Theory of Brillouin Zones"* (1937) under supervision of Eugene Wigner

Herring criterium is routinely used in crystallography for analysis of magnetic and crystal structures

# Herring criterium for classification of irreducible representations (irreps) of the space groups

$$\eta = \frac{l_k}{n(G^0)} \sum_{\substack{h \\ h\mathbf{k} \infty -\mathbf{k}}} \chi^{\kappa\nu}(g^2) = \begin{cases} 1, & \text{if } d^{\kappa\nu} \text{ is real,} \\ 0, & \text{if } d^{\kappa\nu} \text{ is complex and } d^{\kappa\nu} \not\sim (d^{\kappa\nu})^*, \\ -1, & \text{if } d^{\kappa\nu} \text{ is complex and } d^{\kappa\nu} \sim (d^{\kappa\nu})^*. \end{cases}$$

$g = \{h|\tau_h\}$

$\chi^{\kappa\nu}$: character

real, type 1

complex, type 3

pseudoreal, type 2

the irreducible representation matrices $d^{kv}$

# Herring criterium for classification of irreducible representations (irreps) of the space groups

$$\eta = \frac{l_k}{n(G^0)} \sum_{\substack{h \\ h\mathbf{k} \sim -\mathbf{k}}} \chi^{\kappa\nu}(g^2) = \begin{cases} 1, & \text{if } d^{\kappa\nu} \text{ is real,} \\ 0, & \text{if } d^{\kappa\nu} \text{ is complex and } d^{\kappa\nu} \not\sim (d^{\kappa\nu})^*, \\ -1, & \text{if } d^{\kappa\nu} \text{ is complex and } d^{\kappa\nu} \sim (d^{\kappa\nu})^*. \end{cases}$$

real, type 1

complex, type 3

pseudoreal, type 2

character

$g=\{h|\tau_h\}$

the irreducible representation matrices $d^{k\nu}$

# Herring criterium for classification of irreducible representations (irreps) of the space groups

$$\eta = \frac{l_k}{n(G^0)} \sum_{\substack{h \\ h\mathbf{k} \backsim -\mathbf{k}}} \chi^{\kappa\nu}(g^2) = \begin{cases} 1, & \text{if } d^{\kappa\nu} \text{ is real,} \\ 0, & \text{if } d^{\kappa\nu} \text{ is complex and } d^{\kappa\nu} \not\backsim (d^{\kappa\nu})^*, \\ -1, & \text{if } d^{\kappa\nu} \text{ is complex and } d^{\kappa\nu} \backsim (d^{\kappa\nu})^*. \end{cases}$$

character

$g = \{h|\tau_h\}$

real, type 1

complex, type 3

pseudoreal, type 2

the irreducible representation matrices $d^{kv}$

# Herring criterium for classification of irreducible representations (irreps) of the space groups

$$\eta = \frac{l_k}{n(G^0)} \sum_{\substack{h \\ h\mathbf{k} \infty -\mathbf{k}}} \chi^{\kappa\nu}(g^2) = \begin{cases} 1, & \text{if } d^{\kappa\nu} \text{ is real,} \\ 0, & \text{if } d^{\kappa\nu} \text{ is complex and } d^{\kappa\nu} \not\sim (d^{\kappa\nu})^*, \\ -1, & \text{if } d^{\kappa\nu} \text{ is complex and } d^{\kappa\nu} \sim (d^{\kappa\nu})^*. \end{cases}$$

character

$g=\{h|\tau_h\}$

real, type 1

complex, type 3

pseudoreal, type 2

the irreducible representation matrices $d^{kv}$

# Herring criterium for classification of irreducible representations (irreps) of the space groups

$$\eta = \frac{l_k}{n(G^0)} \sum_{\substack{h \\ h\mathbf{k} \infty -\mathbf{k}}} \chi^{\kappa\nu}(g^2) = \begin{cases} 1, & \text{if } d^{\kappa\nu} \text{ is real,} \\ 0, & \text{if } d^{\kappa\nu} \text{ is complex and } d^{\kappa\nu} \not\sim (d^{\kappa\nu})^*, \\ -1, & \text{if } d^{\kappa\nu} \text{ is complex and } d^{\kappa\nu} \sim (d^{\kappa\nu})^*. \end{cases}$$

real, type 1

complex, type 3

pseudoreal, type 2

character

$g=\{h|\tau_h\}$

the irreducible representation matrices $d^{kv}$

Type3: Making use of the condition that quantities of physics must be real, the basis $\psi^{kv}$ of the representation $d^{kv}$ must be joined with the basis $(\psi^{kv})^*$ of the representation $(d^{kv})^*$ Such a reducible representation $d^{kv} \oplus (d^{kv})^*$ is termed irreducible in terms of physics.

# finding unknown complex conjugated (c.c) irrep

**c.c** is NOT always literal **c.c** of $d(g)$

complex conjugated irrep is

$$d^{c.c}(g) = [d(g_0 g g_0^{-1})]^*$$

where $g_0$ is element which transforms the arm **k** into the arm −**k**,

irreps of $G_k$

# finding unknown complex conjugated (c.c) irrep

**c.c** is NOT always literal **c.c** of $d(g)$

complex conjugated irrep is

$$d^{c.c}(g) = [d(g_0 g g_0^{-1})]^*$$

where $g_0$ is element which transforms the arm **k** into the arm −**k**,

irreps of $G_k$

P4/nmm (129) **k**1=[0½w]

| symop (g) | $W_1(0\star)$ | $W_3(0)$ |
|---|---|---|
| $1(t_1,t_2,t_3)$ | $e^{i\pi(t2+2t3\cdot w)}$ | $e^{i\pi(t2+2t3\cdot w)}$ |
| {2_z\|½½0} | 1 | −1 |
| {m_x\|½00} | 1 | 1 |
| {m_y\|0½0} | 1 | −1 |

W3 is **c.c** for W1, η=0, type=3
$g_0$ is −1

---

★η=-1,0,1: pseudo-real, complex, real

# finding unknown complex conjugated (c.c) irrep

**c.c** is NOT always literal **c.c** of $d(g)$

complex conjugated irrep is

$$d^{c.c}(g) = [d(g_0 g g_0^{-1})]^*$$

where $g_0$ is element which transforms the arm **k** into the arm −**k**,

irreps of $G_k$

P4/nmm (129) **k**1=[0½w]

| symop (g) | $W_1(0^\star)$ | $W_3(0)$ |
|---|---|---|
| $1(t_1,t_2,t_3)$ | $e^{i\pi(t2+2t3\cdot w)}$ | $e^{i\pi(t2+2t3\cdot w)}$ |
| {2_z\|½½0} | 1 | −1 |
| {m_x\|½00} | 1 | 1 |
| {m_y\|0½0} | 1 | −1 |

W3 is **c.c** for W1, η=0, type=3
$g_0$ is −1

P6_5 (170) **k**1=[⅓⅓½]

| symop (g) | $H_1(-1)$ | $H_2(0)$ | $H_3(0)$ |
|---|---|---|---|
| 1 | 1 | 1 | |
| $\{3^+\|00⅔\}$ | 1 | $e^{i2\pi/3}$ | $e^{-i2\pi/3}$ |
| $\{3^-\|00⅓\}$ | −1 | $e^{i\pi/3}$ | $e^{-i\pi/3}$ |

$H_1$ is complex but identical to its c.c.
$H_2$ is **c.c.** for $H_3$
$g_0$ is $2_{001}$

P3c1 (158) **k**1=[⅓⅓½]

| symop (g) | $H_1(-1)$ | $H_2(-1)$ | $H_3(-1)$ |
|---|---|---|---|
| 1 | 1 | 1 | 1 |
| $\{3^+\|000\}$ | 1 | $e^{i2\pi/3}$ | $e^{-i2\pi/3}$ |
| $\{3^-\|000\}$ | 1 | $e^{-i2\pi/3}$ | $e^{i2\pi/3}$ |

All three irreps are complex but identical to themselves η=−1, type=2.
$g_0$ is $m_{110}$

---

★η=-1,0,1: pseudo-real, complex, real

# representation approach to the magnetic structure in $Tb_{14}Ag_{51}$

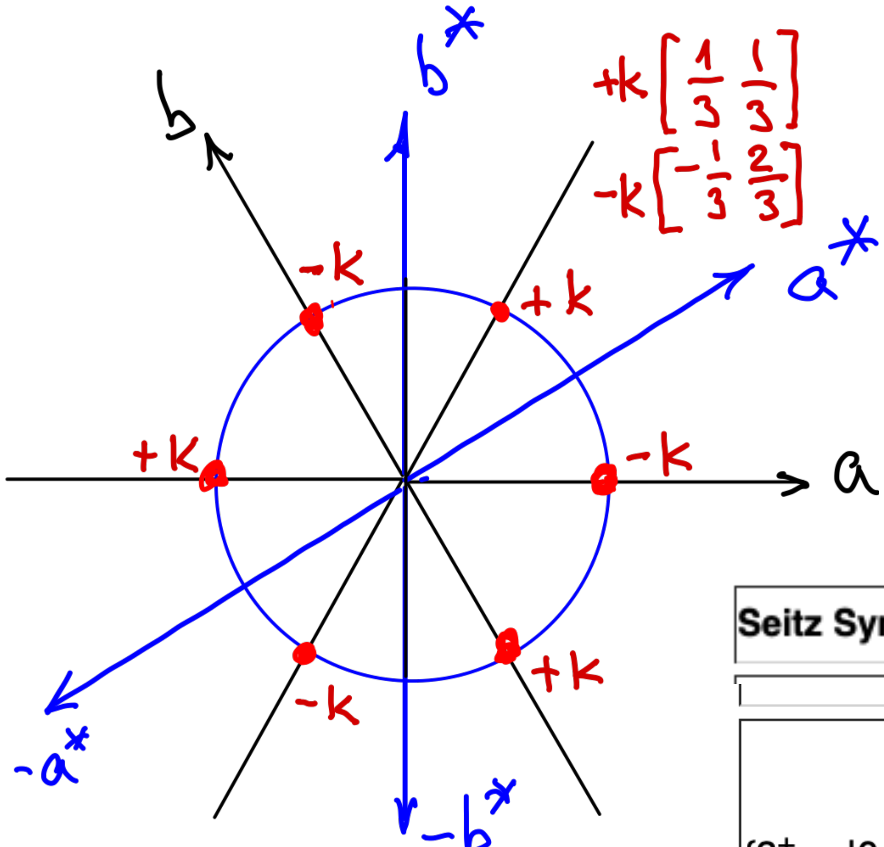


Space group G: 175 P6/m C6h−1
Propagation vector K−point of BZ, k=[1/3,1/3,0]
irreps of the of the little group of propagation vector Gk

| | η=1 | η=1 | η=0 | η=0 | η=0 | η=0 |
|---|---|---|---|---|---|---|
| Seitz Symbol | $K_1$ | $K_2$ | $K_3$ | $K_4$ | $K_5$ | $K_6$ |
| $\{3^{+}_{001}\|0,0,0\}$ | 1 | 1 | $e^{i2\pi/3}$ | $e^{i2\pi/3}$ | $e^{-i2\pi/3}$ | $e^{-i2\pi/3}$ |
| $\{3^{-}_{001}\|0,0,0\}$ | 1 | 1 | $e^{-i2\pi/3}$ | $e^{-i2\pi/3}$ | $e^{i2\pi/3}$ | $e^{i2\pi/3}$ |
| $\{m_{001}\|0,0,0\}$ | 1 | -1 | 1 | -1 | 1 | -1 |

# representation approach to the magnetic structure in Tb14Ag51

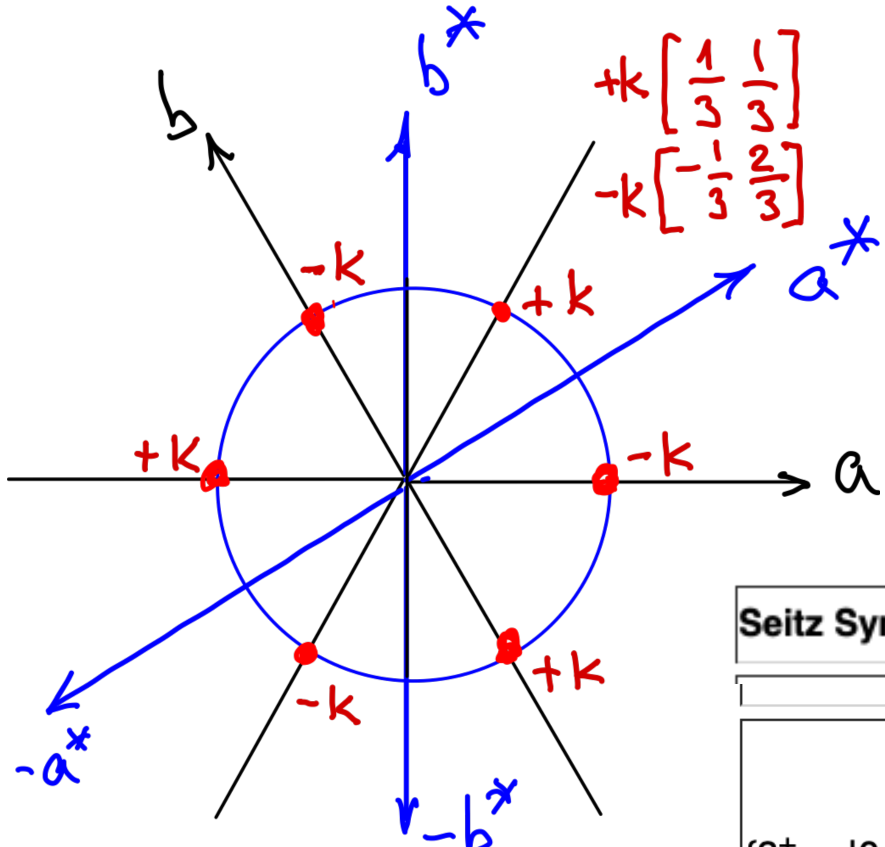


Space group G: 175 P6/m C6h−1
Propagation vector K−point of BZ, k=[1/3,1/3,0]
irreps of the of the little group of propagation vector Gk

| | η=1 | η=1 | η=0 | η=0 | η=0 | η=0 |
|---|---|---|---|---|---|---|
| **Seitz Symbol** | $K_1$ | $K_2$ | $K_3$ | $K_4$ | $K_5$ | $K_6$ |
| $\{3^+_{001}\|0,0,0\}$ | 1 | 1 | $e^{i2\pi/3}$ | $e^{i2\pi/3}$ | $e^{-i2\pi/3}$ | $e^{-i2\pi/3}$ |
| $\{3^-_{001}\|0,0,0\}$ | 1 | 1 | $e^{-i2\pi/3}$ | $e^{-i2\pi/3}$ | $e^{i2\pi/3}$ | $e^{i2\pi/3}$ |
| $\{m_{001}\|0,0,0\}$ | 1 | -1 | 1 | -1 | 1 | -1 |

# representation approach to the magnetic structure in Tb14Ag51

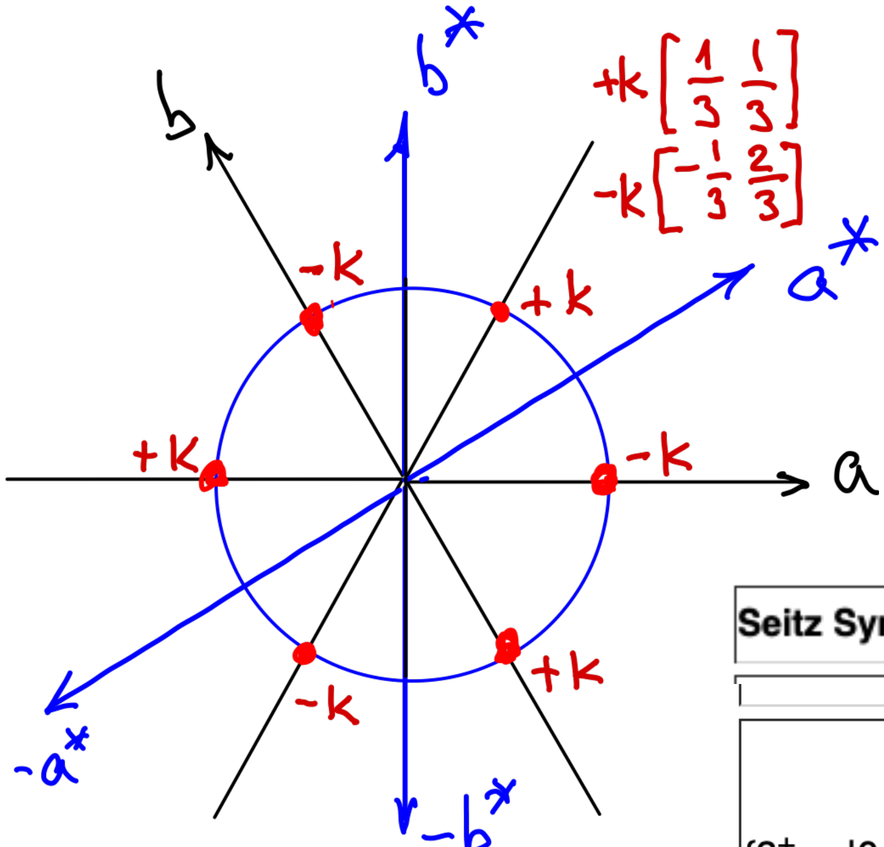


Space group G: 175 P6/m C6h−1
Propagation vector K−point of BZ, k=[1/3,1/3,0]
irreps of the of the little group of propagation vector Gk

| | η=1 | η=1 | η=0 | η=0 | η=0 | η=0 |
|---|---|---|---|---|---|---|
| **Seitz Symbol** | $K_1$ | $K_2$ | $K_3$ | $K_4$ | $K_5$ | $K_6$ |
| $\{3^+_{001}\|0,0,0\}$ | 1 | 1 | $e^{i2\pi/3}$ | $e^{i2\pi/3}$ | $e^{-i2\pi/3}$ | $e^{-i2\pi/3}$ |
| $\{3^-_{001}\|0,0,0\}$ | 1 | 1 | $e^{-i2\pi/3}$ | $e^{-i2\pi/3}$ | $e^{i2\pi/3}$ | $e^{i2\pi/3}$ |
| $\{m_{001}\|0,0,0\}$ | 1 | -1 | 1 | -1 | 1 | -1 |

complex conjugated c.c
η=0 (type=3)

# For complex irrep (η=0) we mix basis functions on the same arm

Hexagonal P6/m space group

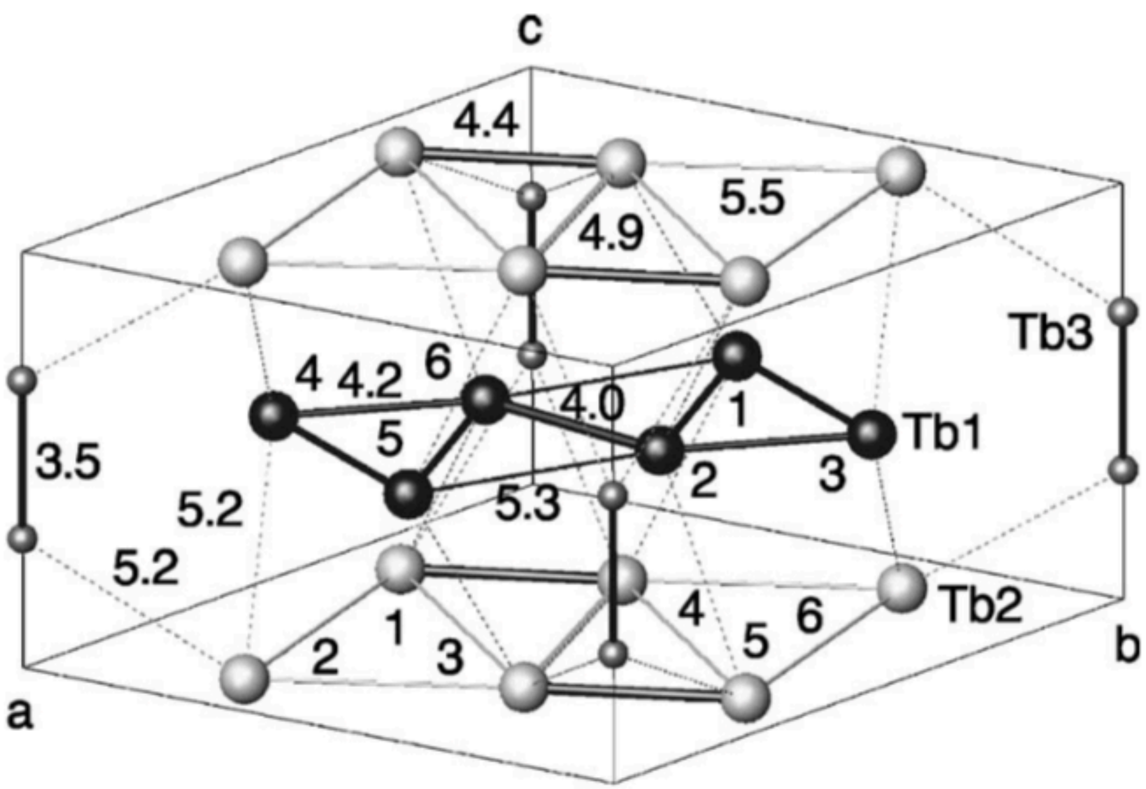


| | |
|---|---|
| Tb1 | 6*k* |
| Tb2 | 6*j* |
| Tb3 | 2*e* |

P6/m (175) **k**=[⅓⅓0]

<u>only irrep K4</u> for Tb1

$\mathbf{m}1 = (mx, my, mz) = C1\cdot(1, \exp(i\pi/3), 0)$

in hex–coordinates is an ideal constant moment **M**(**r**) cycloid

$\mathbf{M}(\mathbf{r}) = \mathrm{Re}\,[\,\mathbf{m}1\cdot\exp(i2\pi(\mathbf{k}\cdot\mathbf{r}))\,]$

$(Mx, My, Mz) = C1\cdot(\cos(\mathbf{k}\cdot\mathbf{r}), \cos(\mathbf{k}\cdot\mathbf{r}+\pi/3), 0)$

# For complex irrep (η=0) we mix basis functions on the same arm

Hexagonal P6/m space group

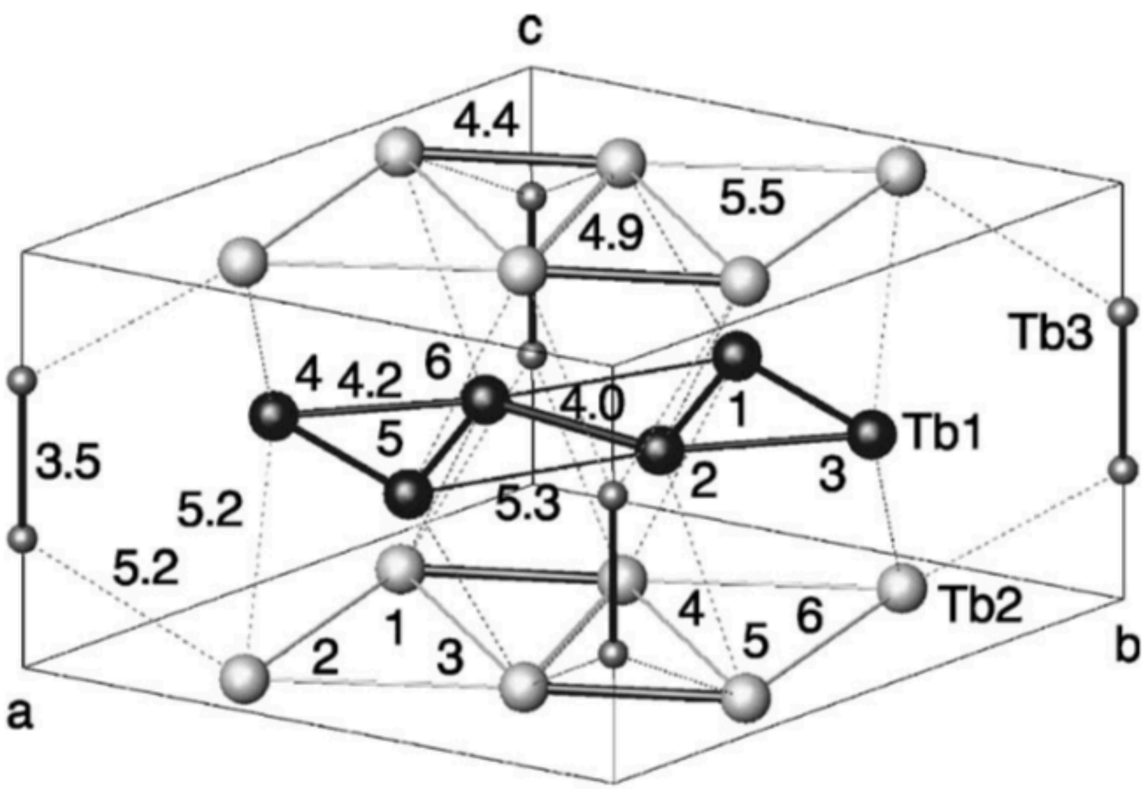


| | |
|---|---|
| Tb1 | 6*k* |
| Tb2 | 6*j* |
| Tb3 | 2*e* |

P6/m (175) **k**=[⅓⅓0]

<u>only irrep K4</u> for Tb1

$\mathbf{m}1 = (mx, my, mz) = C1\cdot(1, \exp(i\pi/3), 0)$

in hex–coordinates is an ideal constant moment **M**(**r**) cycloid

$\mathbf{M}(\mathbf{r}) = \mathrm{Re}\,[\,\mathbf{m}1\cdot\exp(i2\pi(\mathbf{k}\cdot\mathbf{r}))\,]$

$(Mx, My, Mz) = C1\cdot(\cos(\mathbf{k}\cdot\mathbf{r}), \cos(\mathbf{k}\cdot\mathbf{r}+\pi/3), 0)$

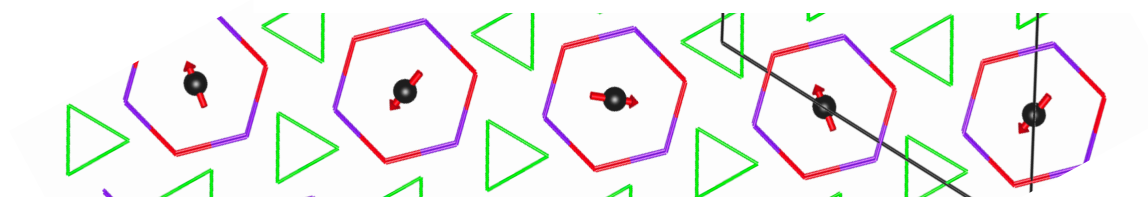

# For complex irrep (η=0) we mix basis functions on the same arm

Hexagonal P6/m space group

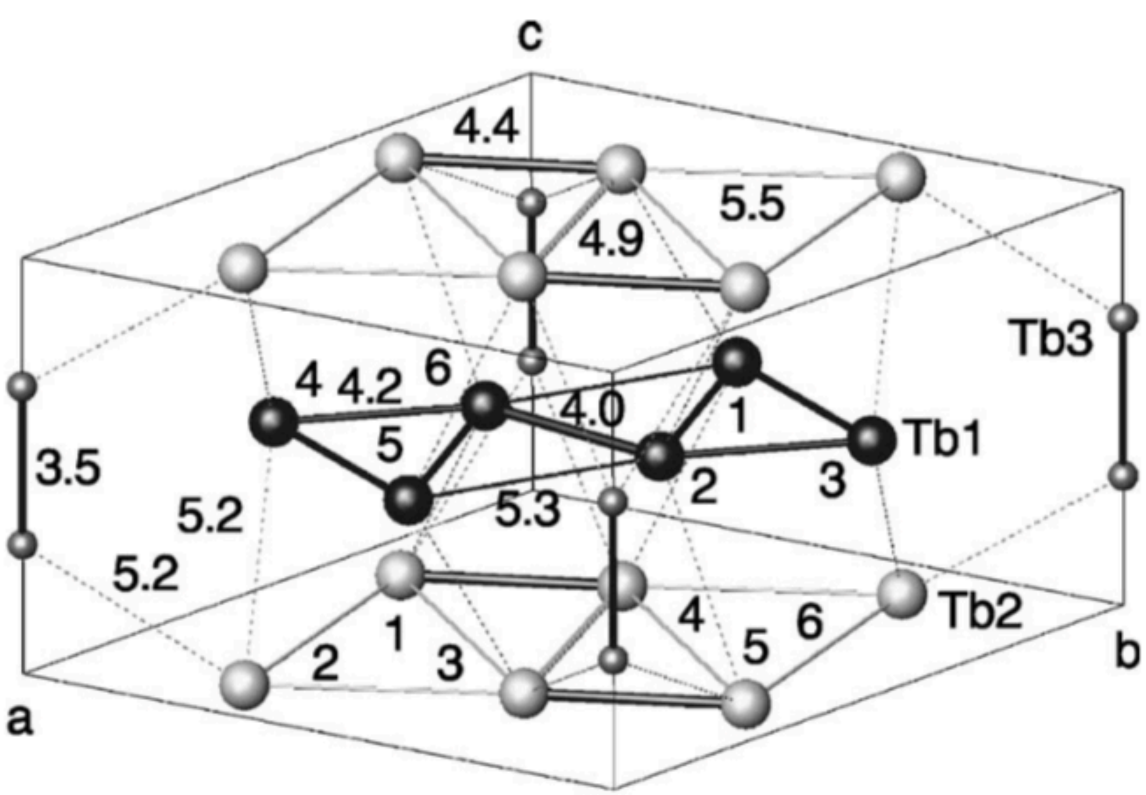


| | |
|---|---|
| Tb1 | 6*k* |
| Tb2 | 6*j* |
| Tb3 | 2*e* |

P6/m (175) **k**=[⅓⅓0]

<u>only irrep K4</u> for Tb1

**m**1 = (mx, my, mz) = C1·(1, exp(i$\pi$/3), 0)

in hex–coordinates is an ideal constant moment **M**(**r**) cycloid

**M**(**r**) = Re [ **m**1·exp(i2$\pi$(**k**·**r**)) ]

(Mx, My, Mz) = C1·(cos(**k**·**r**), cos(**k**·**r**+$\pi$/3), 0)

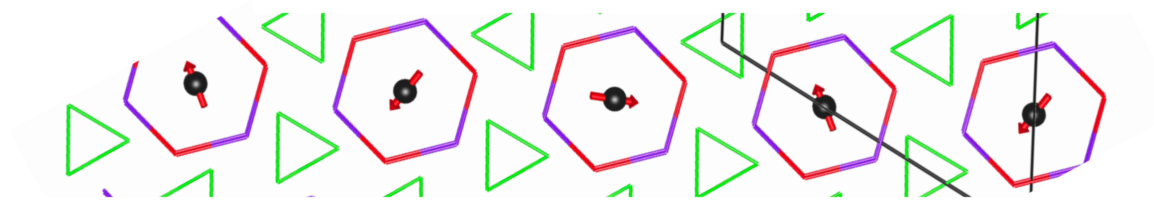

<u>full irrep irrep K4K6</u>

we have to mix two basis functions:

**m**1 = (mx, my, mz) = C1·(1, exp(+i$\pi$/3), 0)

**m**2 = (mx, my, mz) = C2·(1, exp(–i$\pi$/3), 0)

BUT…

we do not know how?

One does not need to know technicalities to determine the magnetic structures and one can use advanced software tools as a black box.

# Web/computer resources to perform group theory symmetry analysis, in particular magnetic structures.

General tools for representation analysis, Shubnikov groups, 3D+n, and much more...

**Two main** web sites with a collection of software which applies group theoretical methods to the analysis of phase transitions in crystalline solids.

Harold T. Stokes, Dorian M. Hatch, and Branton J. Campbell

ISODISTORT: ISOTROPY Software Suite http://iso.byu.edu

→ **ISOTROPY Software Suite**

Harold T. Stokes, Dorian M. Hatch, and Branton J. Campbell, Department of Physics and Astronomy, Brigham Young University, Provo, Utah 84606, USA,

M. I. Aroyo, J. M. Perez–Mato, D. Orobengoa, E. Tasci, G. de la Flor, and A. Kirov

Bilbao Crystallographic Server http://www.cryst.ehu.es/

→ **bilbao crystallographic server**

# Four dimensional irrep that generate the magnetic structure in Tb14Ag51

Space group G: 175 P6/m C6h-1
Propagation vector K−point of BZ, k=[1/3,1/3,0]

Pair of conjugated **non−equivalent** irreps for little group $G_k$ IR

| | | K4 | K6 |
|---|---|---|---|
| $\begin{pmatrix} 0 & -1 & 0 & 0 \\ 1 & -1 & 0 & 0 \\ 0 & 0 & 1 & 0 \end{pmatrix}$ | $\{3^{+}_{001}\|0,0,0\}$ | $e^{i2\pi/3}$ | $e^{-i2\pi/3}$ |
| $\begin{pmatrix} -1 & 1 & 0 & 0 \\ -1 & 0 & 0 & 0 \\ 0 & 0 & 1 & 0 \end{pmatrix}$ | $\{3^{-}_{001}\|0,0,0\}$ | $e^{-i2\pi/3}$ | $e^{i2\pi/3}$ |
| $\begin{pmatrix} -1 & 0 & 0 & 0 \\ 0 & -1 & 0 & 0 \\ 0 & 0 & 1 & 0 \end{pmatrix}$ | $\{2_{001}\|0,0,0\}$ | | |

# Four dimensional irrep that generate the magnetic structure in Tb14Ag51

Space group G: 175 P6/m C6h-1
Propagation vector K−point of BZ, k=[1/3,1/3,0]

| | | Pair of conjugated **non−equivalent** irreps for little group $G_k$ IR | | G IR |
|---|---|---|---|---|
| | | K4 | K6 | K4 |
| $\begin{pmatrix} 0 & -1 & 0 & 0 \\ 1 & -1 & 0 & 0 \\ 0 & 0 & 1 & 0 \end{pmatrix}$ | $\{3^+_{001}\|0,0,0\}$ | $e^{i2\pi/3}$ | $e^{-i2\pi/3}$ | $\begin{pmatrix} e^{i2\pi/3} & 0 \\ 0 & e^{i2\pi/3} \end{pmatrix}$ |
| $\begin{pmatrix} -1 & 1 & 0 & 0 \\ -1 & 0 & 0 & 0 \\ 0 & 0 & 1 & 0 \end{pmatrix}$ | $\{3^-_{001}\|0,0,0\}$ | $e^{-i2\pi/3}$ | $e^{i2\pi/3}$ | $\begin{pmatrix} e^{-i2\pi/3} & 0 \\ 0 & e^{-i2\pi/3} \end{pmatrix}$ |
| $\begin{pmatrix} -1 & 0 & 0 & 0 \\ 0 & -1 & 0 & 0 \\ 0 & 0 & 1 & 0 \end{pmatrix}$ | $\{2_{001}\|0,0,0\}$ | | | $\begin{pmatrix} 0 & -1 \\ -1 & 0 \end{pmatrix}$ |

# Four dimensional irrep that generate the magnetic structure in Tb14Ag51

Space group G: 175 P6/m C6h-1
Propagation vector K−point of BZ, k=[1/3,1/3,0]

| | | Pair of conjugated **non−equivalent** irreps for little group $G_k$ IR: K4 | K6 | G IR: K4 | mK4K6 PIR=IR |
|---|---|---|---|---|---|
| $\begin{pmatrix} 0 & -1 & 0 & 0 \\ 1 & -1 & 0 & 0 \\ 0 & 0 & 1 & 0 \end{pmatrix}$ | $\{3^{+}_{001}\|0,0,0\}$ | $e^{i2\pi/3}$ | $e^{-i2\pi/3}$ | $\begin{pmatrix} e^{i2\pi/3} & 0 \\ 0 & e^{i2\pi/3} \end{pmatrix}$ | $\begin{pmatrix} -1/2 & 0 & \sqrt{3}/2 & 0 \\ 0 & -1/2 & 0 & -\sqrt{3}/2 \\ -\sqrt{3}/2 & 0 & -1/2 & 0 \\ 0 & \sqrt{3}/2 & 0 & -1/2 \end{pmatrix}$ |
| $\begin{pmatrix} -1 & 1 & 0 & 0 \\ -1 & 0 & 0 & 0 \\ 0 & 0 & 1 & 0 \end{pmatrix}$ | $\{3^{-}_{001}\|0,0,0\}$ | $e^{-i2\pi/3}$ | $e^{i2\pi/3}$ | $\begin{pmatrix} e^{-i2\pi/3} & 0 \\ 0 & e^{-i2\pi/3} \end{pmatrix}$ | $\begin{pmatrix} -1/2 & 0 & -\sqrt{3}/2 & 0 \\ 0 & -1/2 & 0 & \sqrt{3}/2 \\ \sqrt{3}/2 & 0 & -1/2 & 0 \\ 0 & -\sqrt{3}/2 & 0 & -1/2 \end{pmatrix}$ |
| $\begin{pmatrix} -1 & 0 & 0 & 0 \\ 0 & -1 & 0 & 0 \\ 0 & 0 & 1 & 0 \end{pmatrix}$ | $\{2_{001}\|0,0,0\}$ | | | $\begin{pmatrix} 0 & -1 \\ -1 & 0 \end{pmatrix}$ | $\begin{pmatrix} 0 & -\sqrt{3}/2 & 0 & -1/2 \\ -\sqrt{3}/2 & 0 & -1/2 & 0 \\ 0 & -1/2 & 0 & \sqrt{3}/2 \\ -1/2 & 0 & \sqrt{3}/2 & 0 \end{pmatrix}$ |

# Four dimensional irrep that generate the magnetic structure in Tb14Ag51

Space group G: 175 P6/m C6h-1
Propagation vector K−point of BZ, k=[1/3,1/3,0]

| | | Pair of conjugated **non−equivalent** irreps for little group $G_k$ IR | | G IR | mK4K6 PIR=IR | Order Parameter direction OPD |
|---|---|---|---|---|---|---|
| | | K4 | K6 | K4 | | |
| $\begin{pmatrix} 0 & -1 & 0 & 0 \\ 1 & -1 & 0 & 0 \\ 0 & 0 & 1 & 0 \end{pmatrix}$ | $\{3^+_{001}\|0,0,0\}$ | $e^{i2\pi/3}$ | $e^{-i2\pi/3}$ | $\begin{pmatrix} e^{i2\pi/3} & 0 \\ 0 & e^{i2\pi/3} \end{pmatrix}$ | $\begin{pmatrix} -1/2 & 0 & \sqrt{3}/2 & 0 \\ 0 & -1/2 & 0 & -\sqrt{3}/2 \\ -\sqrt{3}/2 & 0 & -1/2 & 0 \\ 0 & \sqrt{3}/2 & 0 & -1/2 \end{pmatrix}$ | $\begin{pmatrix} a \\ b \\ c \\ d \end{pmatrix}$ |
| $\begin{pmatrix} -1 & 1 & 0 & 0 \\ -1 & 0 & 0 & 0 \\ 0 & 0 & 1 & 0 \end{pmatrix}$ | $\{3^-_{001}\|0,0,0\}$ | $e^{-i2\pi/3}$ | $e^{i2\pi/3}$ | $\begin{pmatrix} e^{-i2\pi/3} & 0 \\ 0 & e^{-i2\pi/3} \end{pmatrix}$ | $\begin{pmatrix} -1/2 & 0 & -\sqrt{3}/2 & 0 \\ 0 & -1/2 & 0 & \sqrt{3}/2 \\ \sqrt{3}/2 & 0 & -1/2 & 0 \\ 0 & -\sqrt{3}/2 & 0 & -1/2 \end{pmatrix}$ | |
| $\begin{pmatrix} -1 & 0 & 0 & 0 \\ 0 & -1 & 0 & 0 \\ 0 & 0 & 1 & 0 \end{pmatrix}$ | $\{2_{001}\|0,0,0\}$ | | | $\begin{pmatrix} 0 & -1 \\ -1 & 0 \end{pmatrix}$ | $\begin{pmatrix} 0 & -\sqrt{3}/2 & 0 & -1/2 \\ -\sqrt{3}/2 & 0 & -1/2 & 0 \\ 0 & -1/2 & 0 & \sqrt{3}/2 \\ -1/2 & 0 & \sqrt{3}/2 & 0 \end{pmatrix}$ | |

# Possible alternative magnetic symmetries if the spin arrangement transforms according to the four-dimensional physically irreducible representation mK4K6.

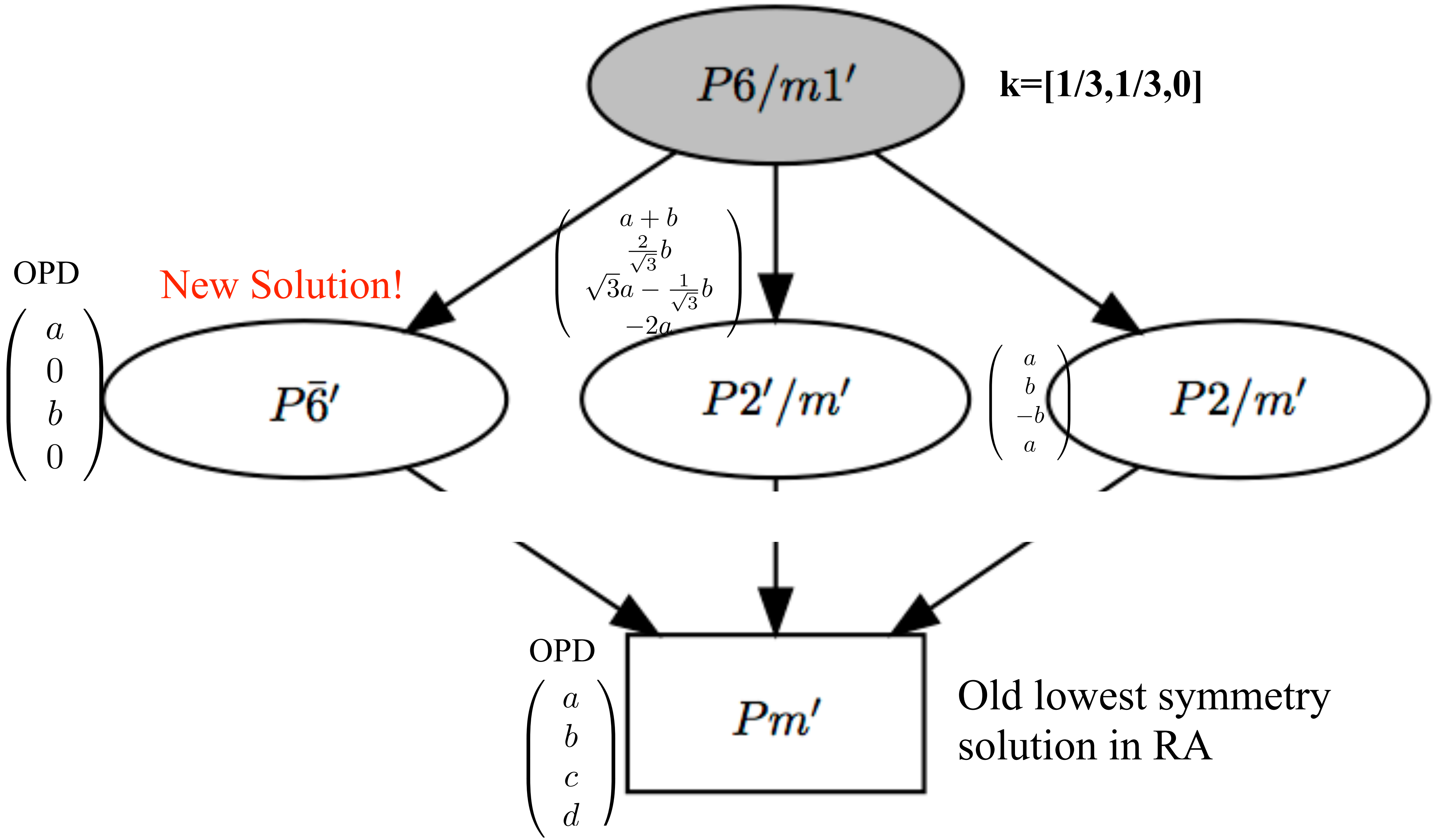

# Possible alternative magnetic symmetries if the spin arrangement transforms according to the four-dimensional physically irreducible representation mK4K6.

1. Restrict the symmetry to hex.
2. In addition to modes of **k=[1/3,1/3,0]** allows modes with **$\mathbf{k_0}$=[0,0,0]**, which is 3rd harmonic of k

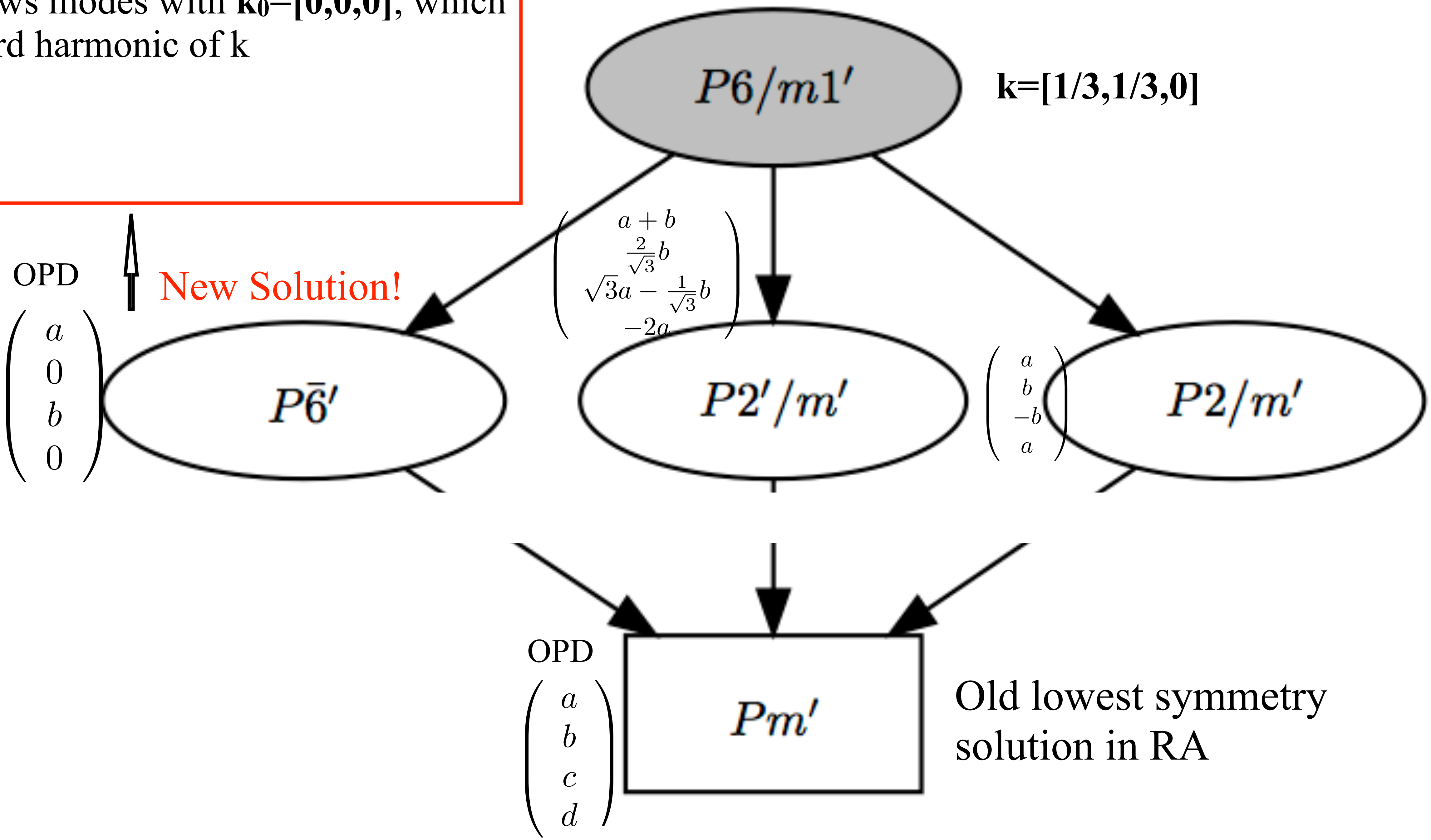

# Possible alternative magnetic symmetries if the spin arrangement transforms according to the four-dimensional physically irreducible representation mK4K6.

1. Restrict the symmetry to hex.
2. In addition to modes of **k=[1/3,1/3,0]** allows modes with **$k_0$=[0,0,0]**, which is 3rd harmonic of k

   One mode mGM1- for Tb3 with **M** || c-axis, and modes of mGM1- and mGM2+ with **M** ⊥ c-axis for Tb1 and Tb2.

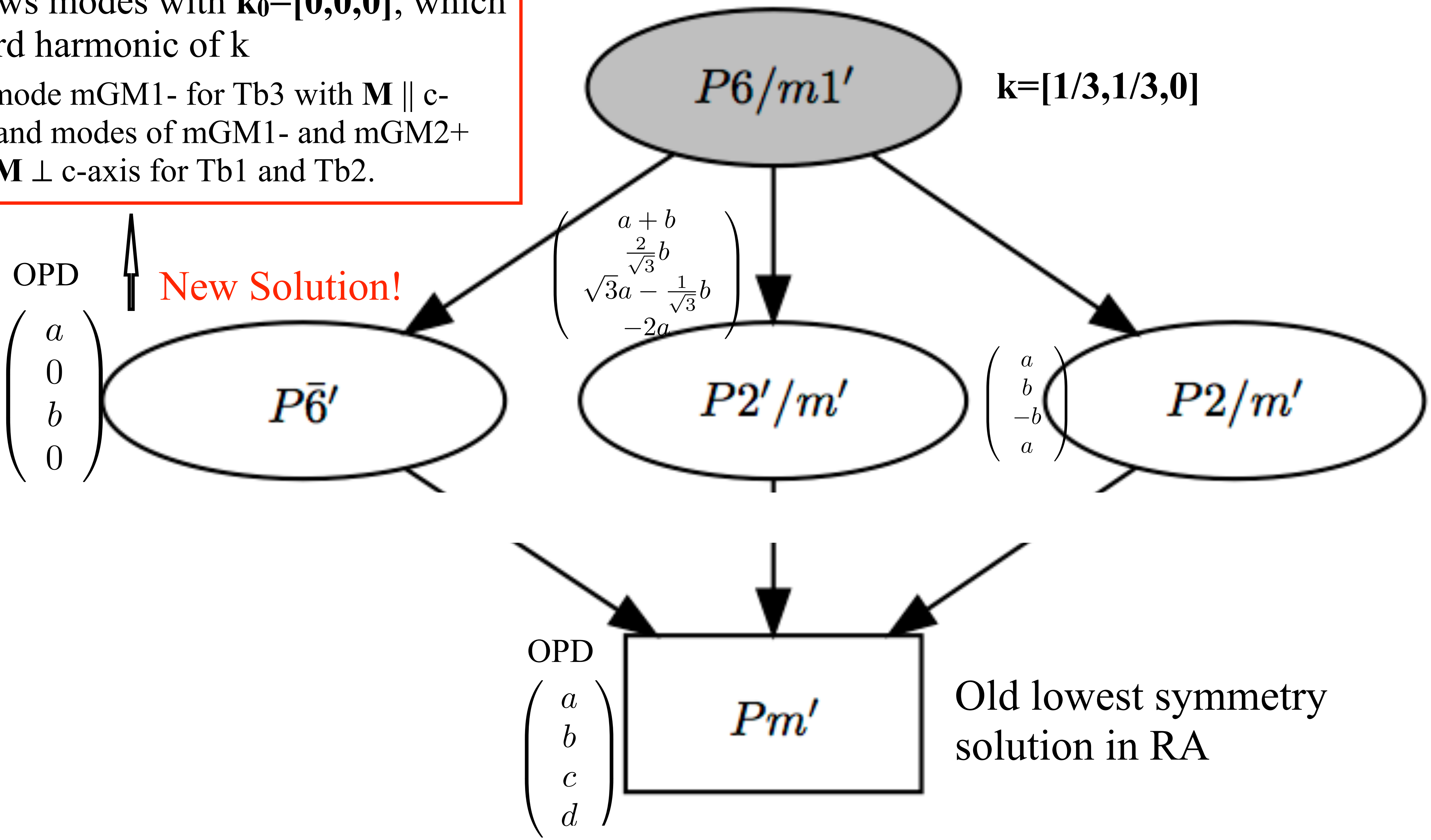

# A note on the relations between irreps and magnetic symmetry

**irrep**: only mK4mK6 k=[1/3,1/3,0] as a primary mode, no $k_0$=[0,0,0]-contribution. Possible to introduce 3rd harmonics $k_0 = 3k$, but symmetry needs to be assigned, which is not trivial.

**magnetic symmetry MSG**: the modes of primary irrep k and and the secondary ones $k_0$ are 'entangled' and add up.

```
TB1_1 -0.88942 -2.72166 0.00000 Mx,My,0
TB1_2  1.04243  4.18925 0.00000 Mx,My,0
TB1_3 -0.15301 -1.46760 0.00000 Mx,My,0
…
```

## An artificial example: if the irrep is pseudo-real (−1) the number of alternative symmetries is smaller than for complex one.

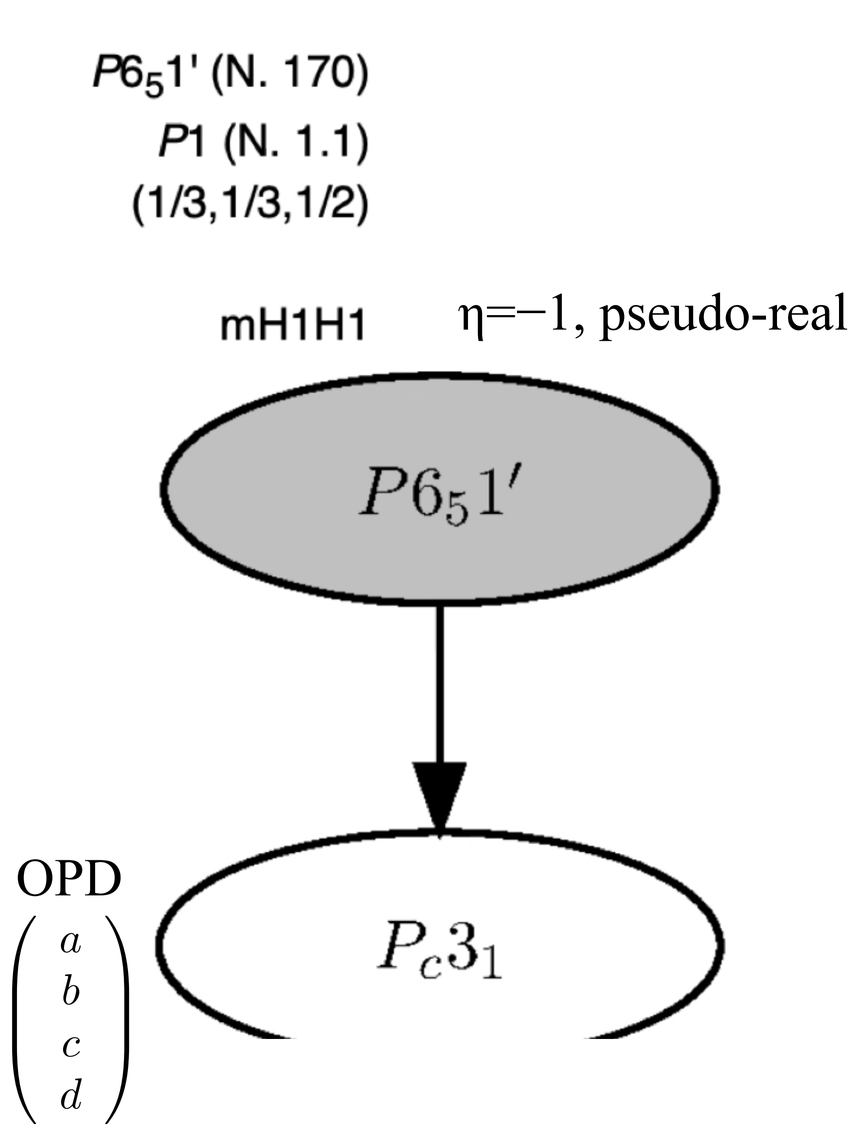


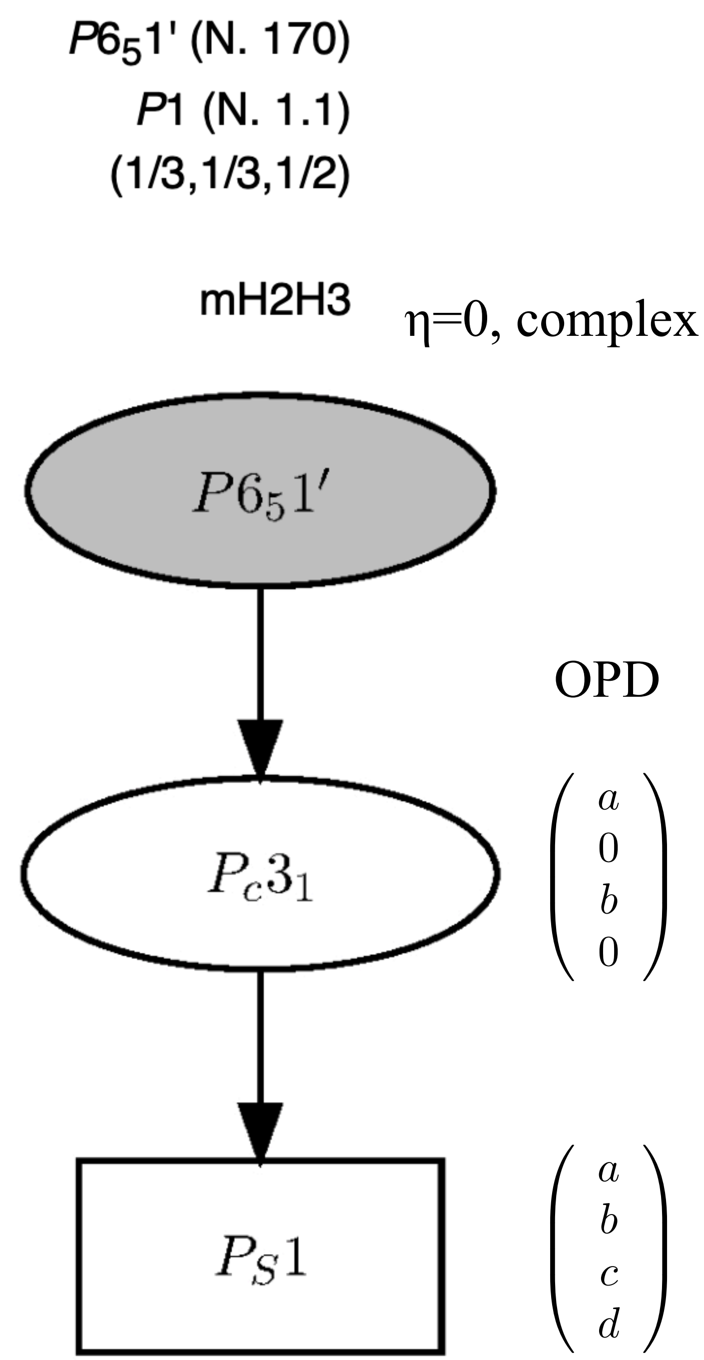

# Neutron diffraction experiments

# Old solution (2006): only k-point, but Pm'

Difference neutron powder diffraction pattern between at T = 1.5 and 30 K.

$R_p$= 7.98, $R_{wp}$= 11.2, $R_{exp}$= 1.31 and $\chi^2$= 73.0

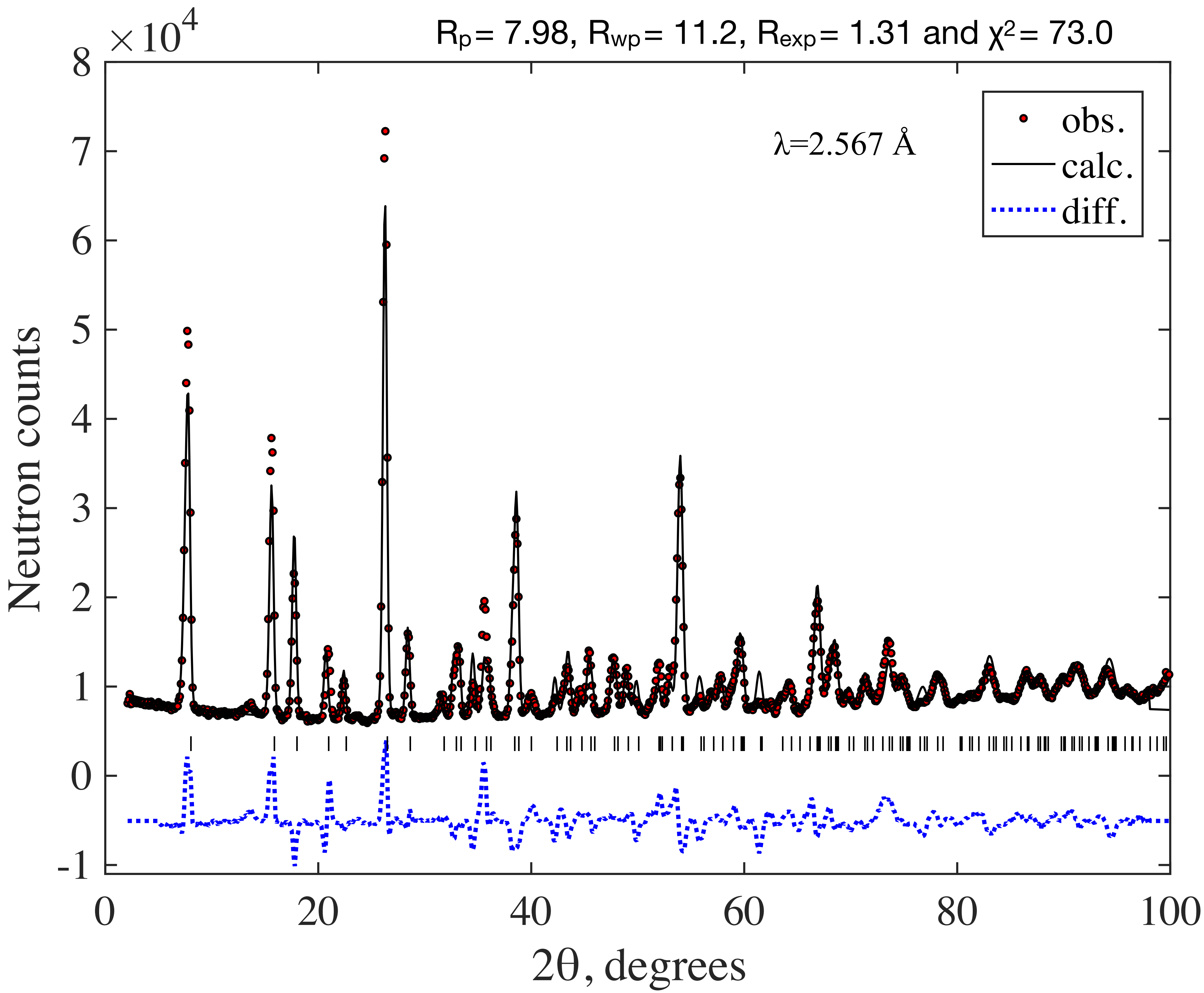

# Old fit (only k-point irrep but arbitrary irrep mix)

Neutron powder diffraction pattern measured at T = 1.5K with wavelength 2.567 Å.
Blue – magnetic contribution.

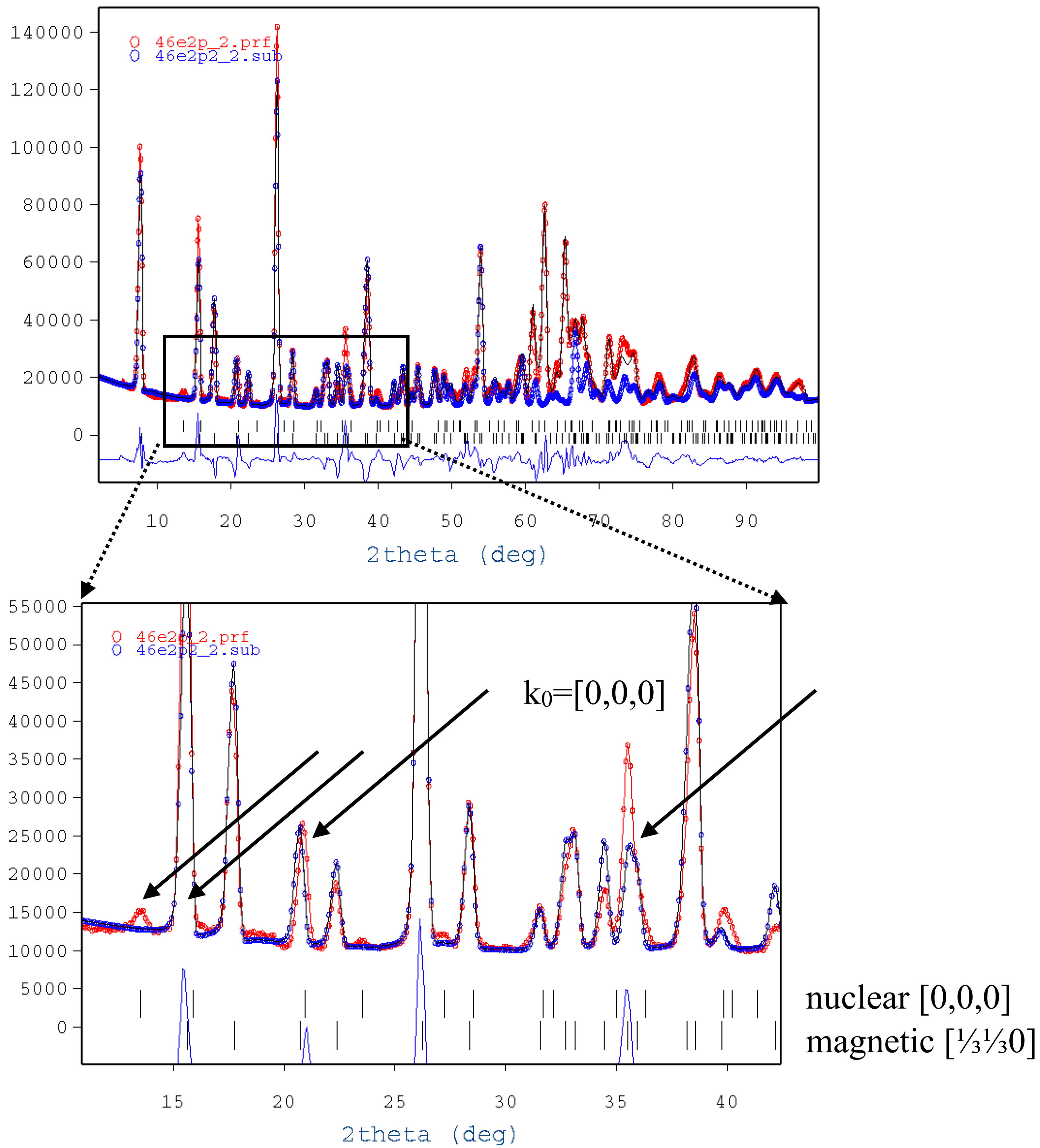

# Le Bail vs. new model

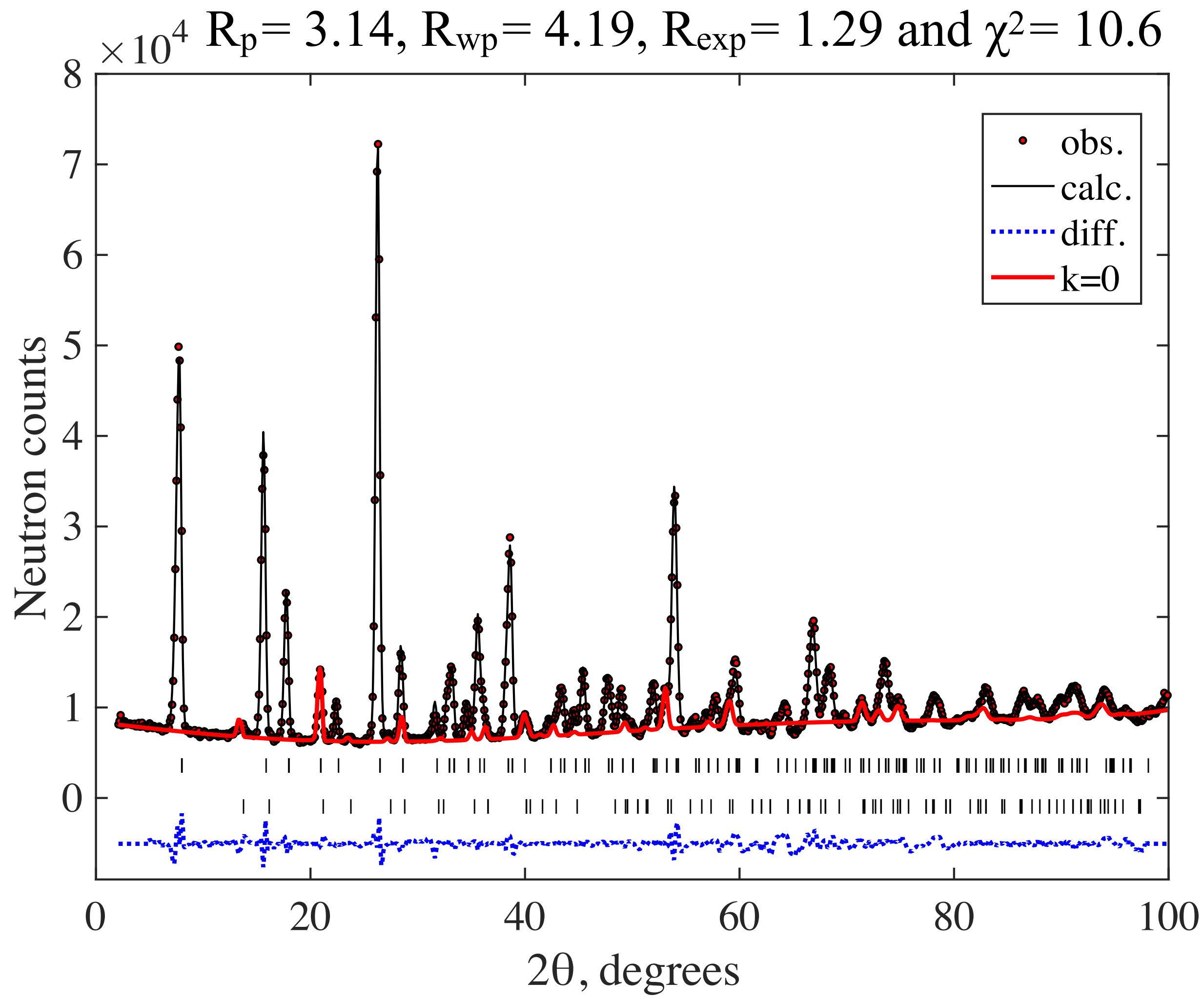


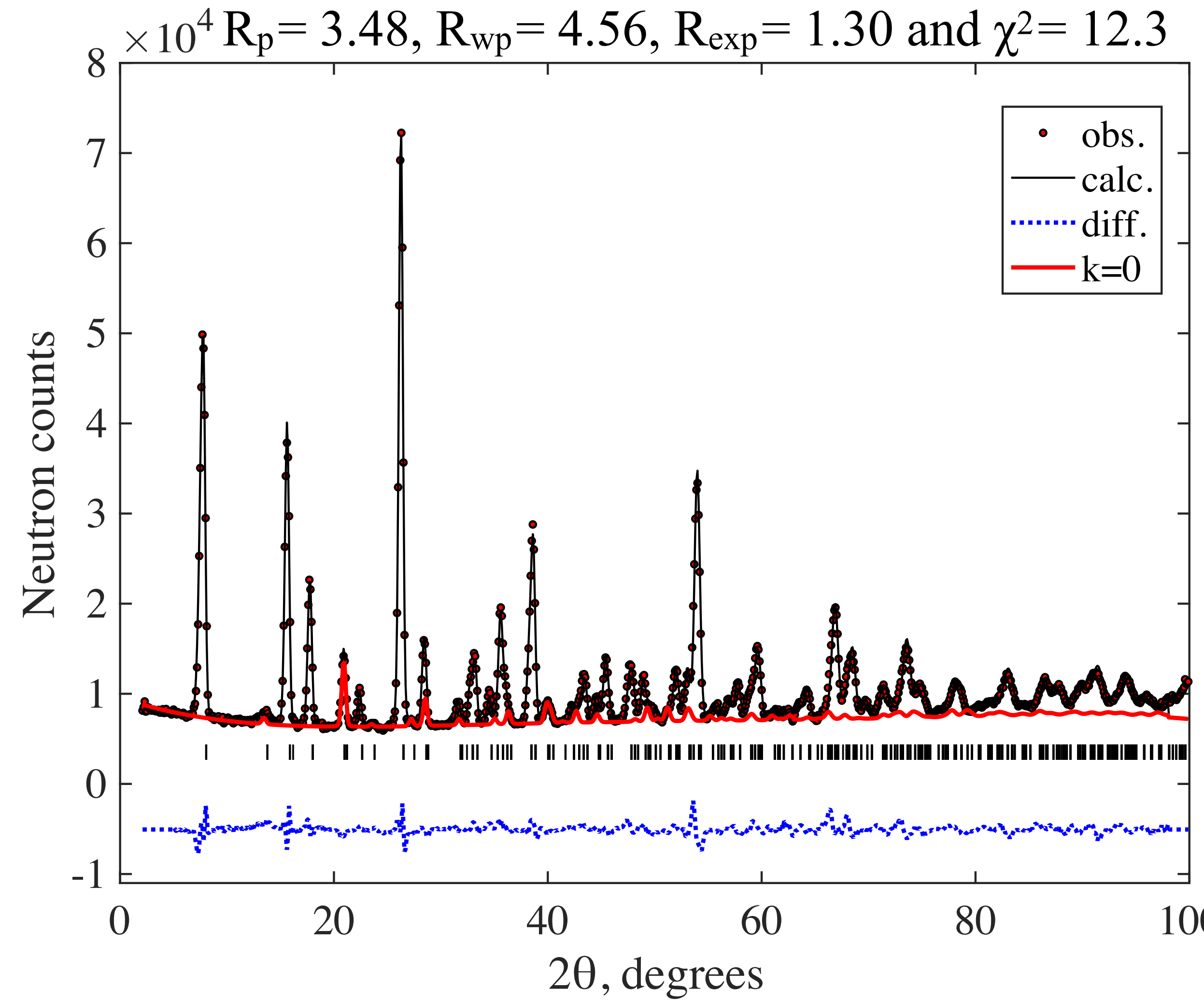


P-6'

27 parameters, which reduce to 15 assuming constant moment

Tb1 6*k* → 6 sites 3k

Tb2 6*j* → 6 sites 3j

Tb3 2*e* → 1 site 6l

78 if only irreps without symmetry

# P-6' AFM structure of Tb14Ag51

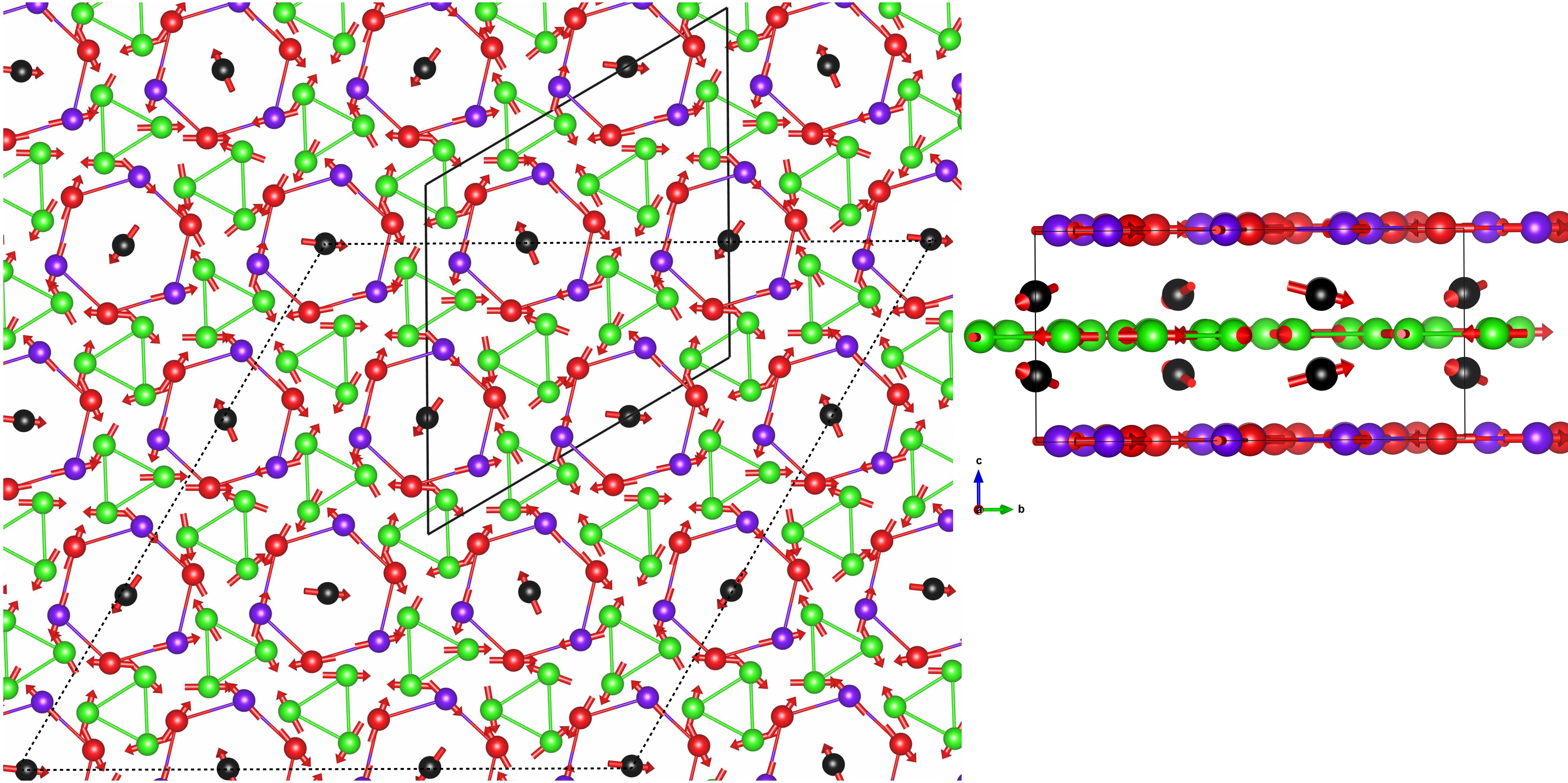


View of the magnetic structure (a) in projection on the xy plane and (b) along the a axis corresponding to the refined model with P6' symmetry. The unit cell is indicated by a black solid line. The dotted line shows a 3a x 3b supercell of the parent space group P6/m. Tb1 atoms are in green forming the triangles and Tb3 atoms are in black at the centres of hexagons. Tb2a_1, Tb2a_2 and Tb2a_3 are in red, and the remaining three atoms derived from the Tb2 site are in blue.

# Decomposition of P-6' AFM structure of Tb14Ag5 into harmonics

It is remarkable that the two modes separately do not maintain a common moment magnitude for all atoms, and this is only attained through the combination of the two contributions

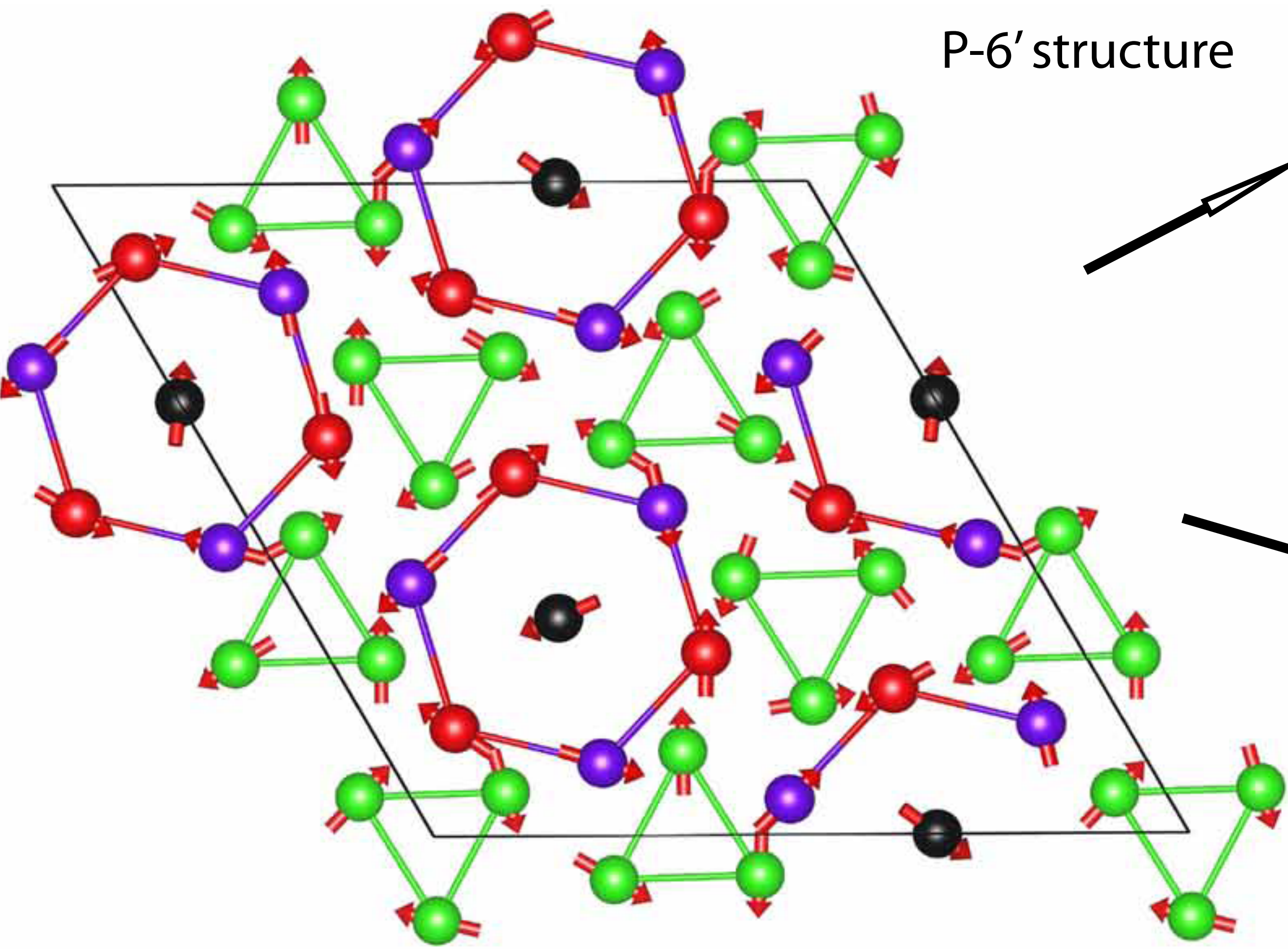


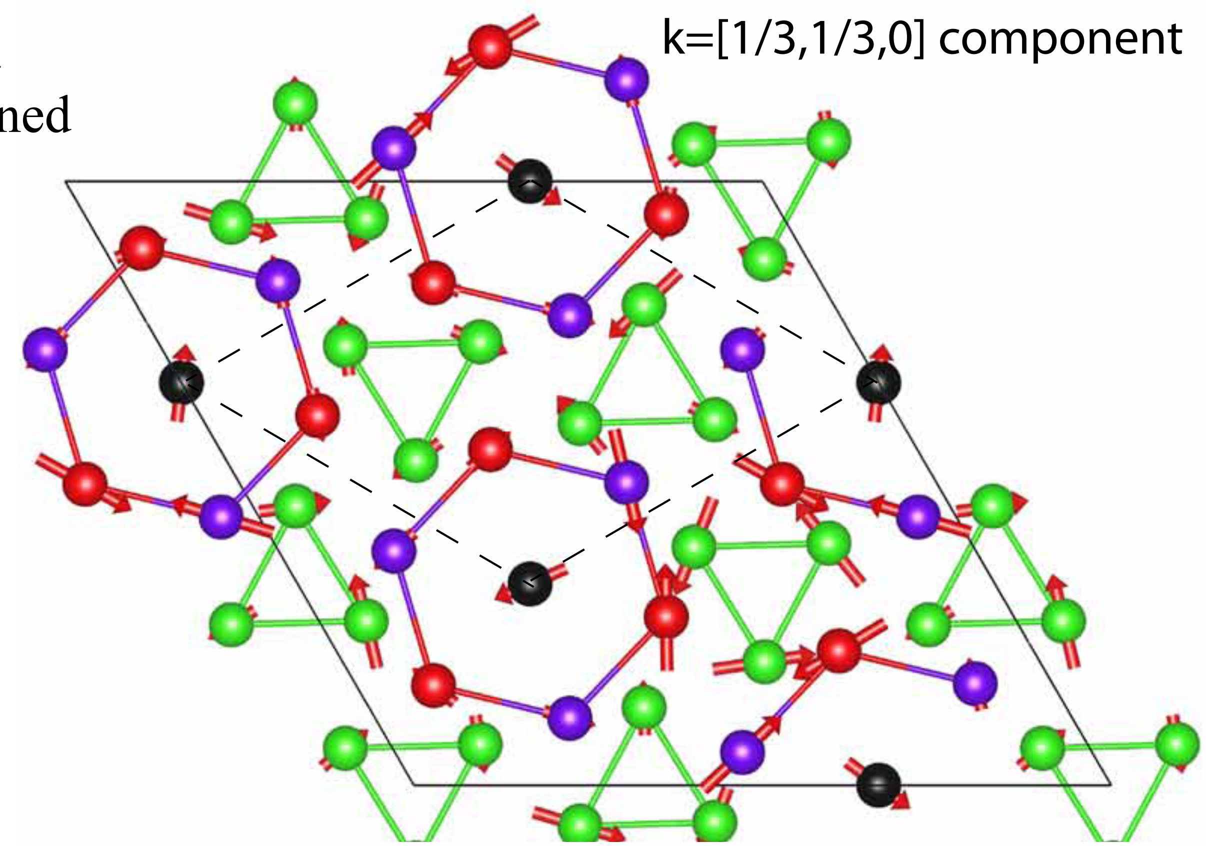


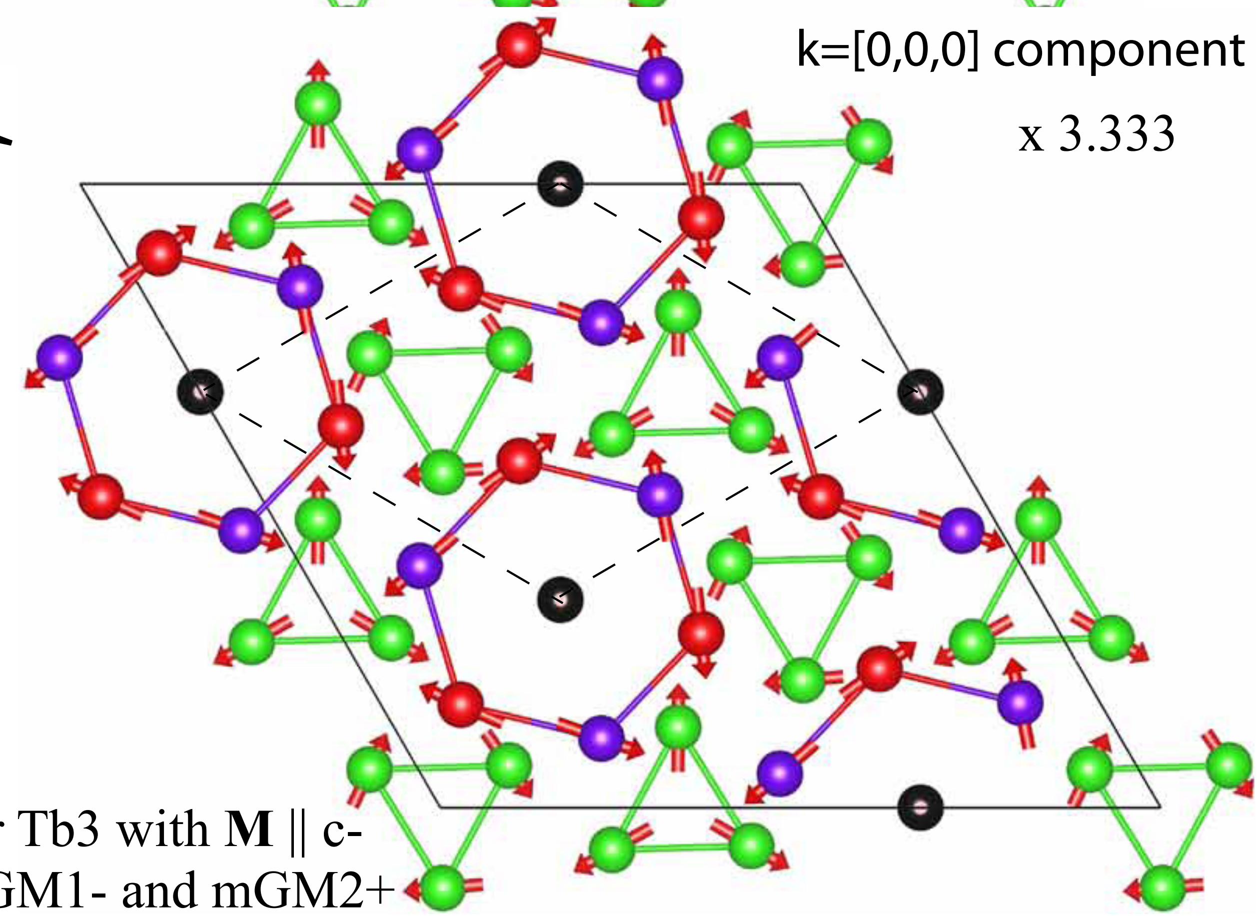


One mode mGM1- for Tb3 with **M** || c-axis, and modes of mGM1- and mGM2+ with **M** ⊥ c-axis for Tb1 and Tb2.

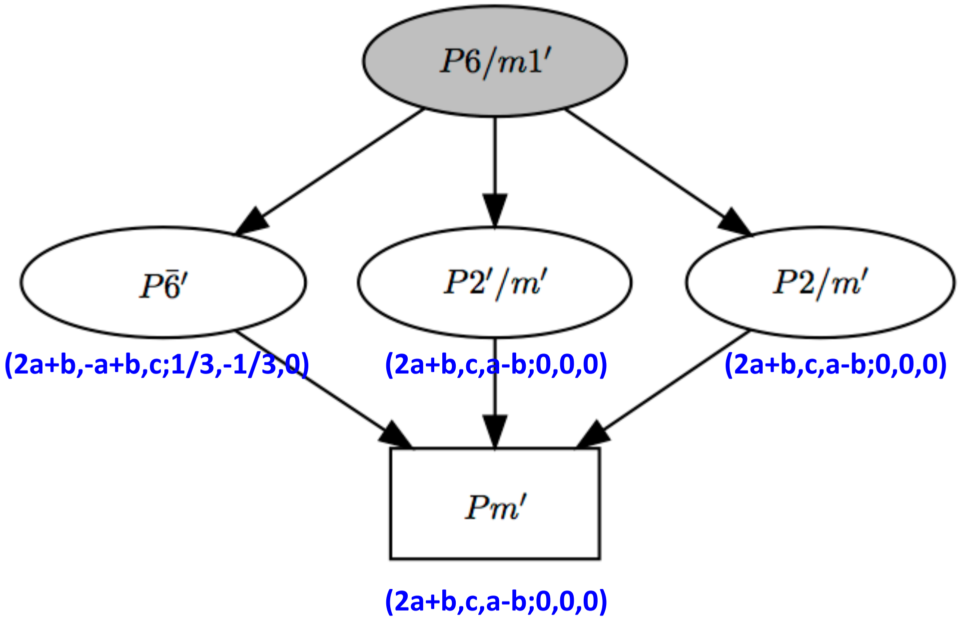


# Conclusions

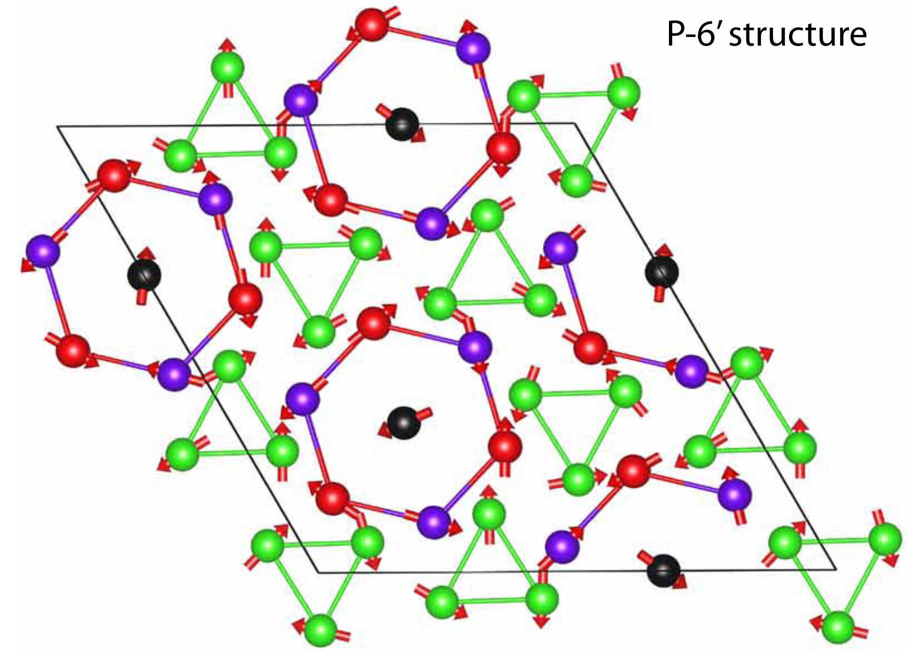


- The antiferromagnetic structure of $Tb_{14}Ag_{51}$ was determined using both magnetic symmetry and irreducible representation arguments.

- The structure given by propagation vector $\mathbf{k}_K$=[1/3,1/3,0] in P6/m is hexagonal magnetic space group (MSG) P-6': maximal possible symmetry for 4D irrep mK4K6.

- P-6' *constrains* the possible mK4K6 ordering that can be present in the structure and implicitly *introduces* third harmonic secondary degrees of freedom associated with propagation vector k = 0 (with weight 34% of $k_K$ ) – the modulation is *not sinusoidal*

- 13 independent Tb magnetic moments, all having the same absolute moment value 8.48 (2) μB. 12 Tb – cycloid at in ab-plane and one substantial additional helical contribution.

**Thank you!**

# A note: If we use only magnetic symmetry without irreps

too many subgroups to consider and we loose the concept of single irrep active at the transition

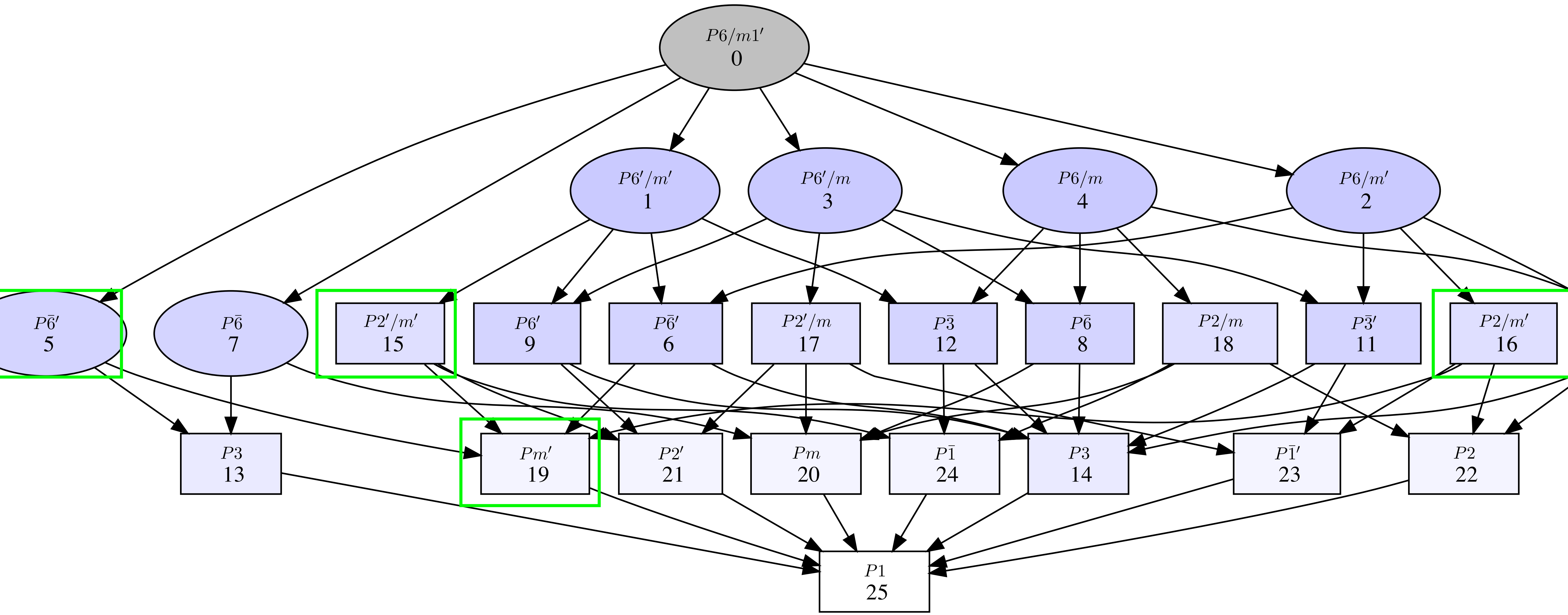

# mK2, etc

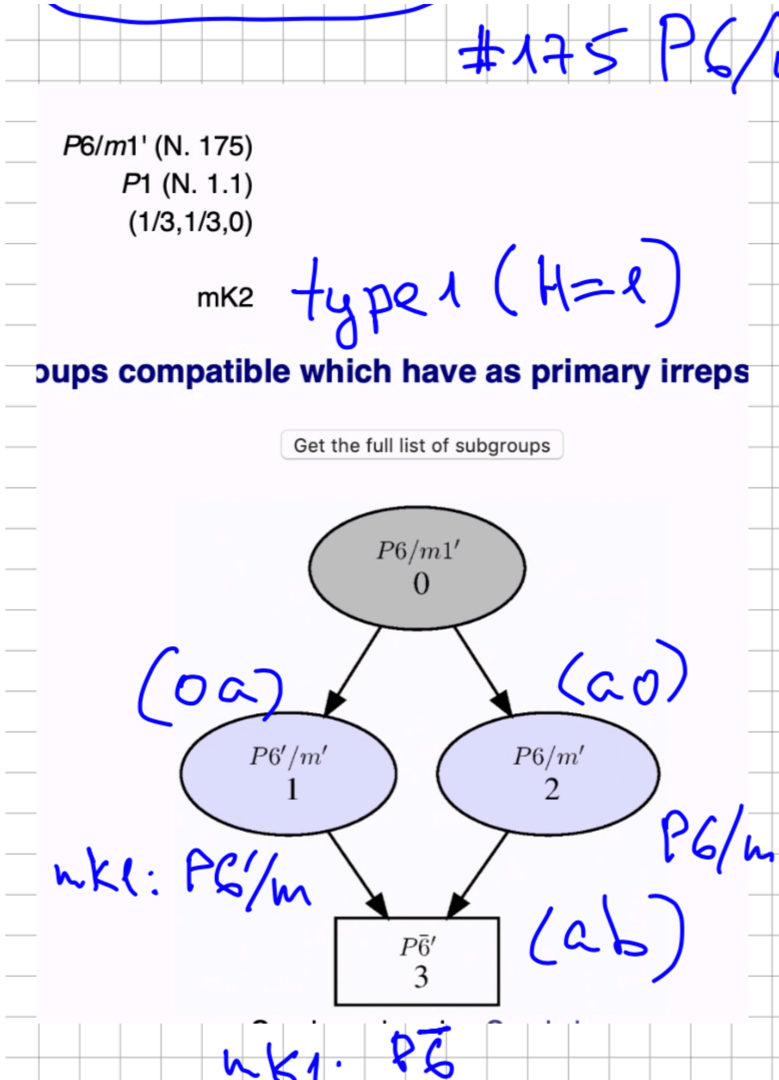


We do not loose high symmetry for 1D ireps of type 1 and 2 (H=1,-1) real, pseudoreal

2D for {k,-k}

but

do loose for H=0

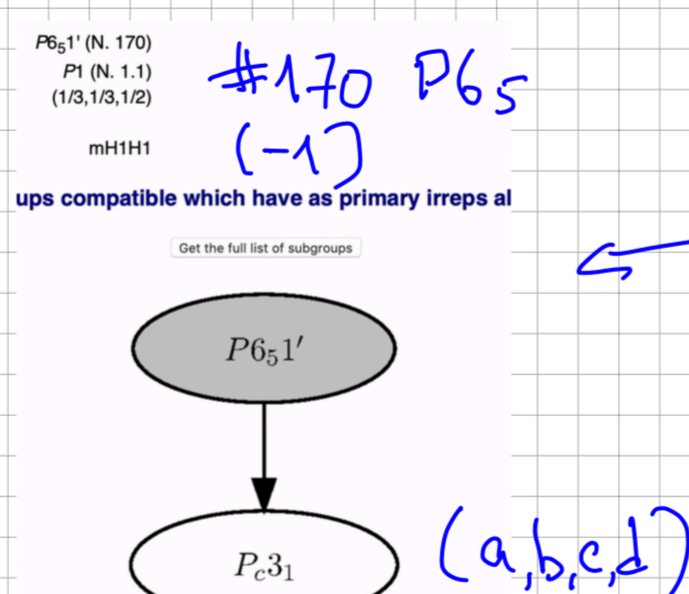


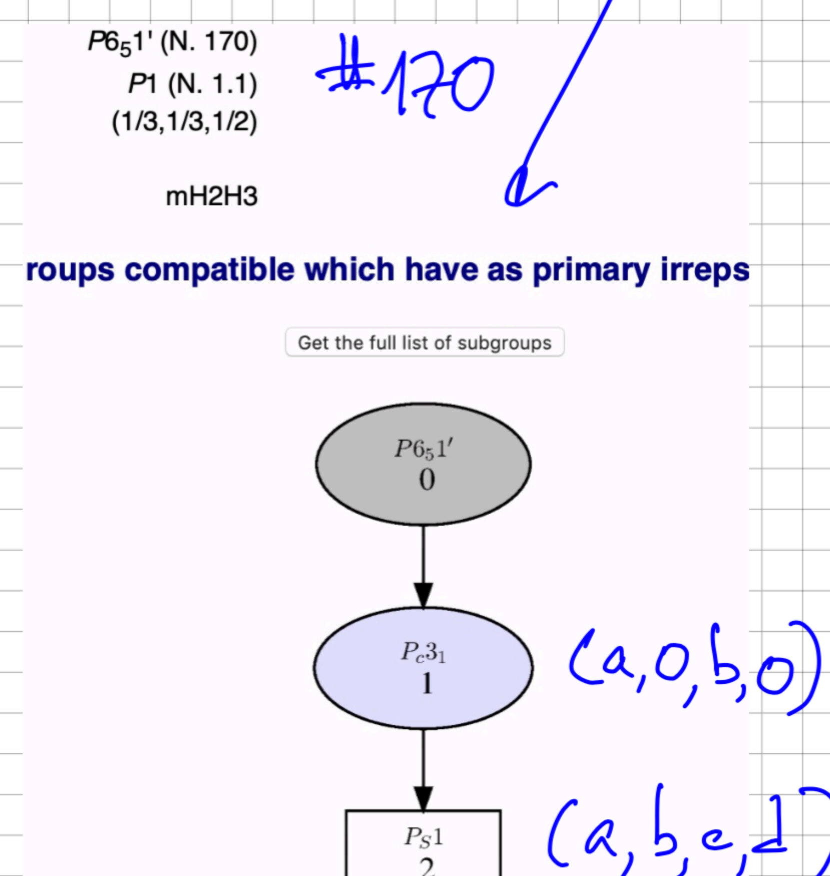

# combined fit of both nuclear and magnetic phase

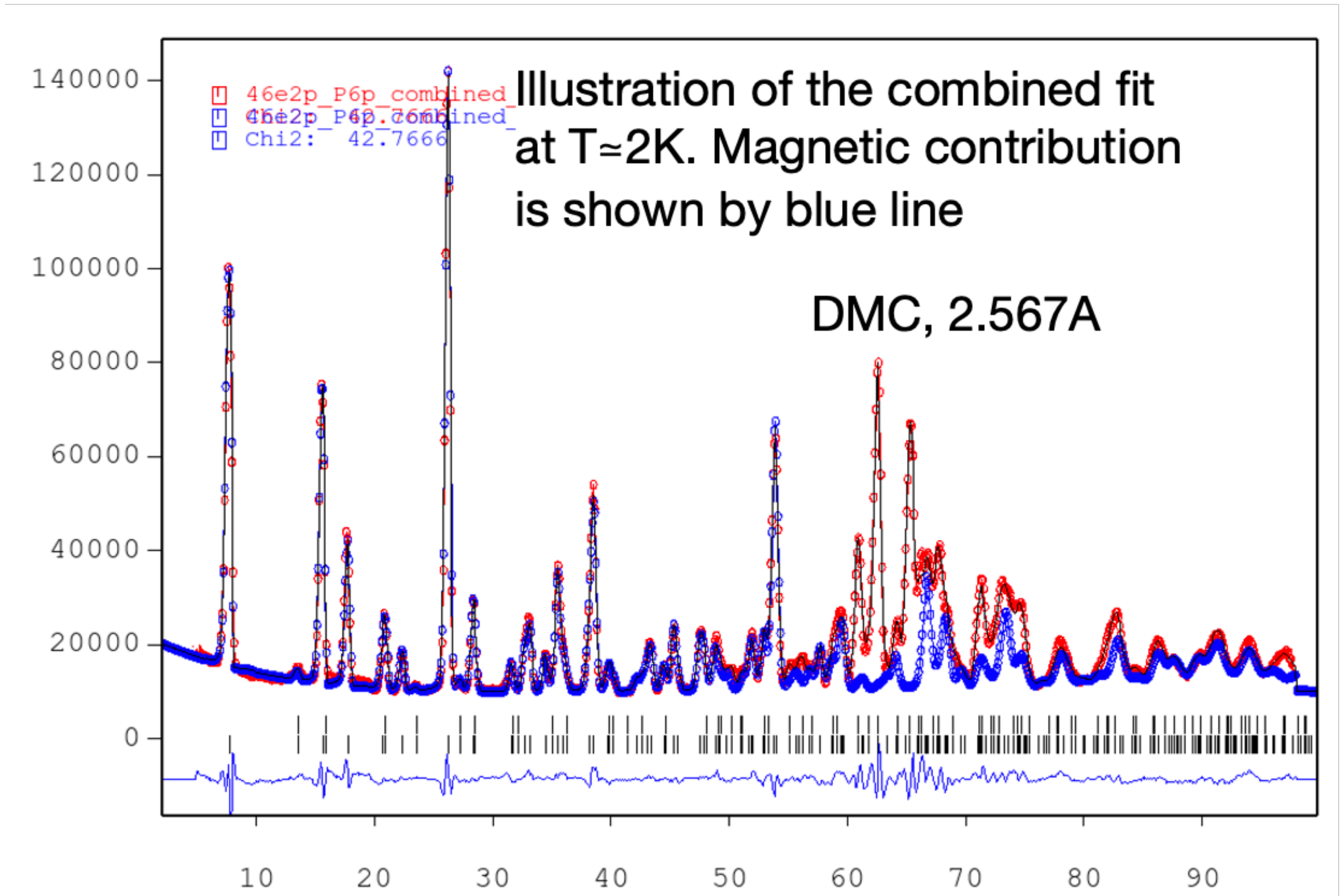


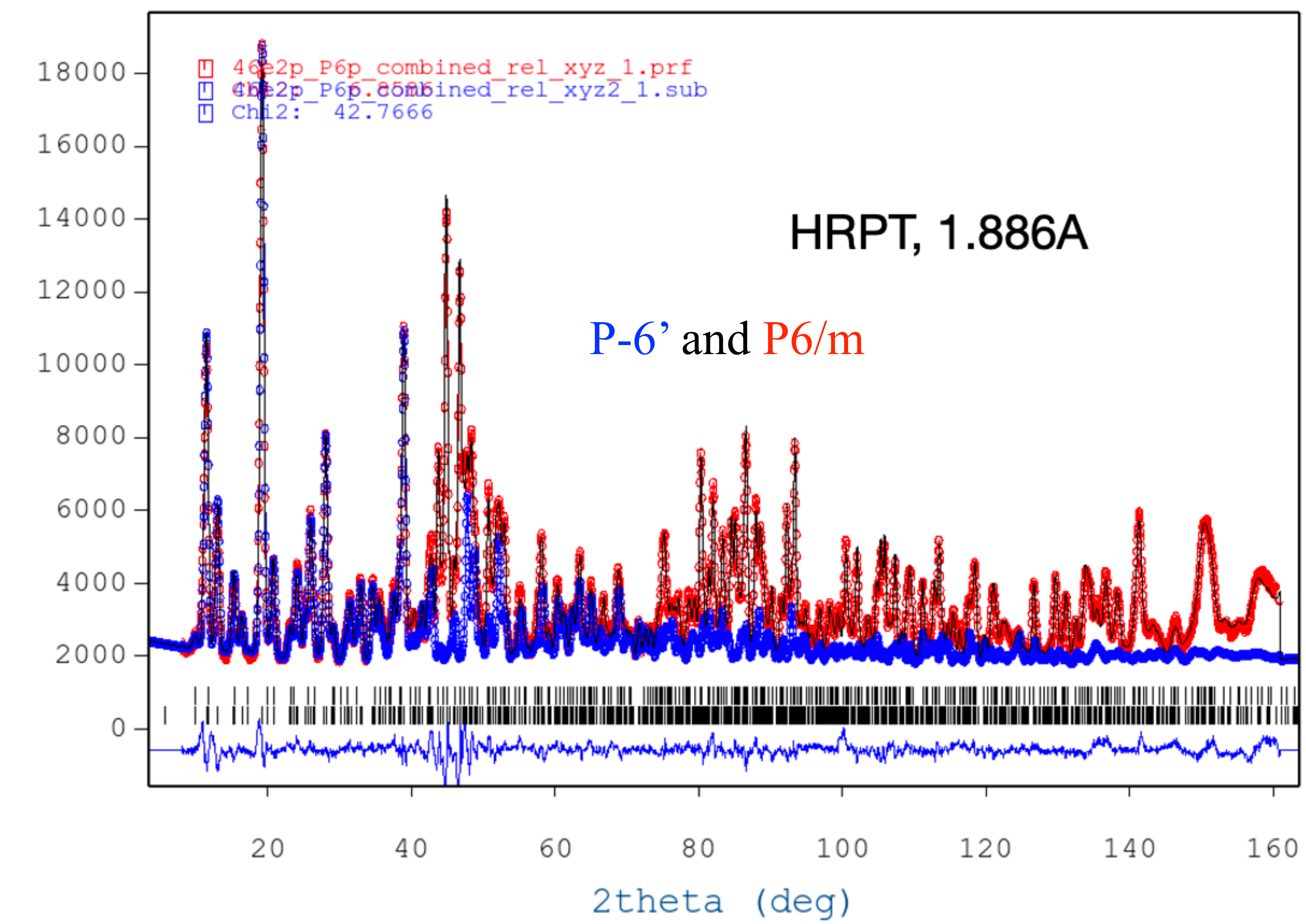


The combined fit with the crystal structure in the space group P6/m converged well, with the atomic positions (19 parameters in total) within less than 1.5 standard deviations from their values in the paramagnetic phase at 30 K for all parameters except four, i.e. 2.3 for x-AG1, 1.9 for y-AG2, 2.0 for y-AG3 and 1.6 for y-AG4. We find these deviations insignificant.

Article | Open Access | Published: 11 September 2020

# Visualization of ferroaxial domains in an order-disorder type ferroaxial crystal

T. Hayashida, Y. Uemura, K. Kimura, S. Matsuoka, D. Morikawa, S. Hirose, K. Tsuda, T. Hasegawa & T. Kimura

*Nature Communications* **11**, Article number: 4582 (2020) | Cite this article



## Abstract

Ferroaxial materials that exhibit spontaneous ordering of a rotational structural distortion with an axial vector symmetry have gained growing interest, motivated by recent extensive studies on ferroic materials. As in conventional ferroics (e.g., ferroelectrics and ferromagnetics), domain states will be present in the ferroaxial materials. However, the observation of ferroaxial domains is non-trivial due to the nature of the order parameter, which is invariant under both time-reversal and space-inversion operations. Here we propose that $NiTiO_3$ is an order-disorder type ferroaxial material, and spatially resolve its ferroaxial domains by using linear electrogyration effect: optical rotation in proportion to an applied electric field. To detect small signals of electrogyration (order of $10^{-5}$ deg $V^{-1}$), we adopt a recently developed difference image-sensing technique. Furthermore, the ferroaxial domains are confirmed on nano-scale spatial resolution with a combined use of scanning transmission electron microscopy and convergent-beam electron diffraction. Our success of the domain visualization will promote the study of ferroaxial materials as a new ferroic state of matter.

he order parameter characterizing ferroaxial materials is a rotational electric-dipole rrangement[1] and represented by a ferroaxial moment (or ferro-rotation moment) **A** defined s $\mathbf{A} \propto \sum_i \mathbf{r}_i \times \mathbf{p}_i$, where $\mathbf{r}_i$ denotes a position vector of electric dipole $\mathbf{p}_i$ from the ymmetrical center of a structural unit[2,3]. For example, **A** is generated by head-to-tail rrangements of electric dipoles as illustrated in Fig. 1a. The **A** is an axial vector invariant nder both time-reversal and spatial-inversion operations though other symmetries such as a nirror parallel to **A** is broken. The ferroaxial order is closely related to various phenomena ncluding magnetoelectric couplings in multiferroics[4,5,6] and polar vortices in anostructured materials[2,7]. Such an order is sometimes called ferro-rotational order[3,8], and hese terms are often used to describe the existence of rotational distortions inducing finite **A** vith or without a phase transition[4,5,6].

**Fig. 1: Ferroaxial order and linear electrogyration induced by ferroaxial order.**

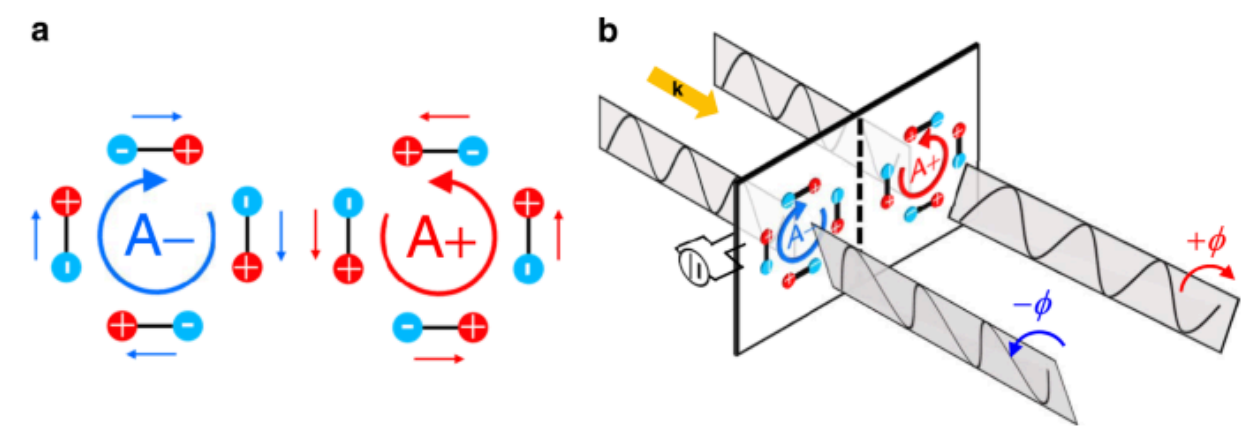


**a** Ferroaxial moment defined as $\mathbf{A} \propto \sum_i \mathbf{r}_i \times \mathbf{p}_i$, which characterizes ferroaxial materials. Here $\mathbf{r}_i$ denotes a position vector of electric dipole $\mathbf{p}_i$ from the symmetrical center of a structural unit. The

| | Symbol | ${}^{*}K_4(0)$ |
|---|---|---|
| $\begin{pmatrix} 1 & 0 & 0 & t_1 \\ 0 & 1 & 0 & t_2 \\ 0 & 0 & 1 & t_3 \end{pmatrix}$ | $\{1\|t_1,t_2,t_3\}$ | $\begin{pmatrix} e^{i2\pi(t_1+t_2)/3} & 0 \\ 0 & e^{-i2\pi(t_1+t_2)/3} \end{pmatrix}$ |
| $\begin{pmatrix} 0 & -1 & 0 & 0 \\ 1 & -1 & 0 & 0 \\ 0 & 0 & 1 & 0 \end{pmatrix}$ | $\{3^{+}_{001}\|0,0,0\}$ | $\begin{pmatrix} e^{i2\pi/3} & 0 \\ 0 & e^{i2\pi/3} \end{pmatrix}$ |
| $\begin{pmatrix} -1 & 1 & 0 & 0 \\ -1 & 0 & 0 & 0 \\ 0 & 0 & 1 & 0 \end{pmatrix}$ | $\{3^{-}_{001}\|0,0,0\}$ | $\begin{pmatrix} e^{-i2\pi/3} & 0 \\ 0 & e^{-i2\pi/3} \end{pmatrix}$ |
| $\begin{pmatrix} -1 & 0 & 0 & 0 \\ 0 & -1 & 0 & 0 \\ 0 & 0 & 1 & 0 \end{pmatrix}$ | $\{2_{001}\|0,0,0\}$ | $\begin{pmatrix} 0 & -1 \\ -1 & 0 \end{pmatrix}$ |
| $\begin{pmatrix} 0 & 1 & 0 & 0 \\ -1 & 1 & 0 & 0 \\ 0 & 0 & 1 & 0 \end{pmatrix}$ | $\{6^{-}_{001}\|0,0,0\}$ | $\begin{pmatrix} 0 & e^{-i\pi/3} \\ e^{-i\pi/3} & 0 \end{pmatrix}$ |
| $\begin{pmatrix} 1 & -1 & 0 & 0 \\ 1 & 0 & 0 & 0 \\ 0 & 0 & 1 & 0 \end{pmatrix}$ | $\{6^{+}_{001}\|0,0,0\}$ | $\begin{pmatrix} 0 & e^{i\pi/3} \\ e^{i\pi/3} & 0 \end{pmatrix}$ |
| $\begin{pmatrix} -1 & 0 & 0 & 0 \\ 0 & -1 & 0 & 0 \\ 0 & 0 & -1 & 0 \end{pmatrix}$ | $\{\bar{1}\|0,0,0\}$ | $\begin{pmatrix} 0 & 1 \\ 1 & 0 \end{pmatrix}$ |
| $\begin{pmatrix} 0 & 1 & 0 & 0 \\ -1 & 1 & 0 & 0 \\ 0 & 0 & -1 & 0 \end{pmatrix}$ | $\{\bar{3}^{+}_{001}\|0,0,0\}$ | $\begin{pmatrix} 0 & e^{i2\pi/3} \\ e^{i2\pi/3} & 0 \end{pmatrix}$ |
| $\begin{pmatrix} 1 & -1 & 0 & 0 \\ 1 & 0 & 0 & 0 \\ 0 & 0 & -1 & 0 \end{pmatrix}$ | $\{\bar{3}^{-}_{001}\|0,0,0\}$ | $\begin{pmatrix} 0 & e^{-i2\pi/3} \\ e^{-i2\pi/3} & 0 \end{pmatrix}$ |
| $\begin{pmatrix} 1 & 0 & 0 & 0 \\ 0 & 1 & 0 & 0 \\ 0 & 0 & -1 & 0 \end{pmatrix}$ | $\{m_{001}\|0,0,0\}$ | $\begin{pmatrix} -1 & 0 \\ 0 & -1 \end{pmatrix}$ |
| $\begin{pmatrix} 0 & -1 & 0 & 0 \\ 1 & -1 & 0 & 0 \\ 0 & 0 & -1 & 0 \end{pmatrix}$ | $\{\bar{6}^{-}_{001}\|0,0,0\}$ | $\begin{pmatrix} e^{-i\pi/3} & 0 \\ 0 & e^{-i\pi/3} \end{pmatrix}$ |
| $\begin{pmatrix} -1 & 1 & 0 & 0 \\ -1 & 0 & 0 & 0 \\ 0 & 0 & -1 & 0 \end{pmatrix}$ | $\{\bar{6}^{+}_{001}\|0,0,0\}$ | $\begin{pmatrix} e^{i\pi/3} & 0 \\ 0 & e^{i\pi/3} \end{pmatrix}$ |

$G_k$ #175 $P6/m$ $k = \frac{1}{3}\frac{1}{3}0$

$+2$

$e^{i2\pi/3}$ $\frac{\sqrt{3}+1)}{2}$ $+ = -2$

$e^{-i2\pi/3}$ $\frac{\sqrt{3}-1)}{2}$

$\chi(g^2)$

$+2$

$\frac{(i\sqrt{3}-1)^2}{2}$ $+ = -2$

$\frac{(i\sqrt{3}+1)^2}{2}$

$+2$

$\frac{(i\sqrt{3}-1)^2}{2}$ $+ = -2$

$\frac{(i\sqrt{3}+1)^2}{2}$

$\eta = 0$

$h(k) = -k$

$-1$ $+2$

$e^{-i\pi/3}$ $\frac{(i\sqrt{3}-1)^2}{2}$ $+ = -2$

$e^{i\pi/3}$ $\frac{\sqrt{3}+1)}{2}$